Deep-Learning-Based Medical Image Synthesis and Its Potential Clinical Applications

Xiaofeng Yang, PhD

Radiation Oncology and Winship Cancer Institute
Emory University, Atlanta, GA

EMORY | WINSHIP CANCER INSTITUTE

Medical Image Synthesis

- With the development of artificial intelligence, especially deep learning, medical image synthesis between different medical imaging modalities/protocols is an active research field with great clinical interest in radiation oncology and radiology.
- Medical image synthesis aims to facilitate a specific clinical workflow by bypassing or replacing a certain imaging procedure when the acquisition is infeasible, costs additional time/labor/expense, has ionizing radiation exposure, or introduces uncertainty from image registration between different modalities.
- The benefit of medical image synthesis has raised increasing interest in a number of potential clinical applications such as MRI-only radiation therapy treatment planning, CBCT-guided adaptive radiotherapy, quantitative PET/MRI imaging, image segmentation, multimodality image registration, high-quality image generation, and etc.

Deep Learning in Medical Image Synthesis (120+ papers)

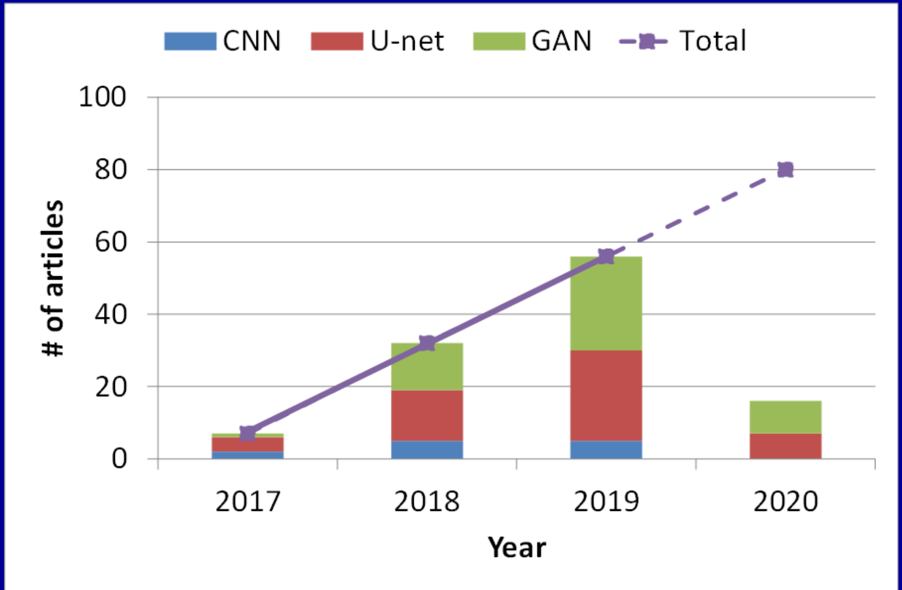

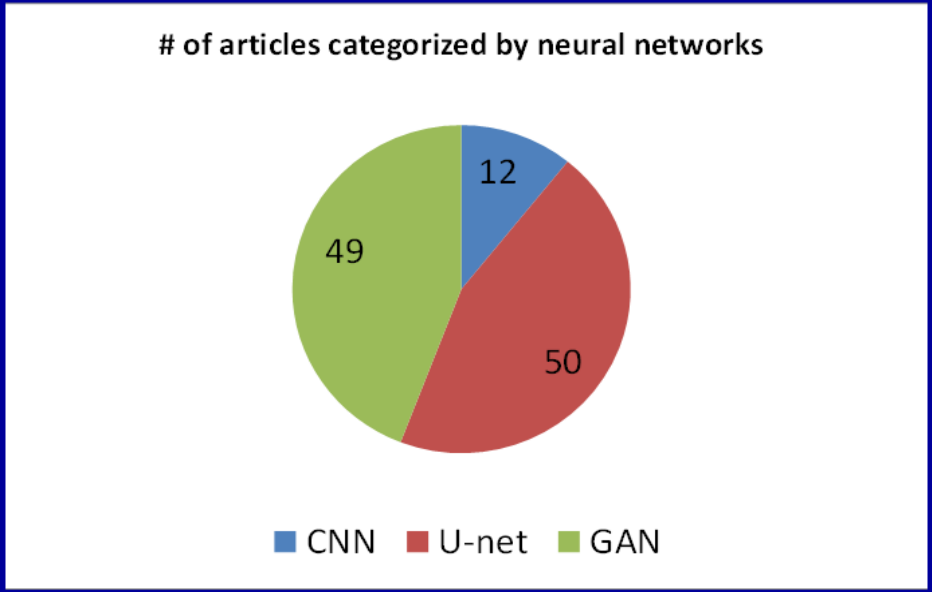

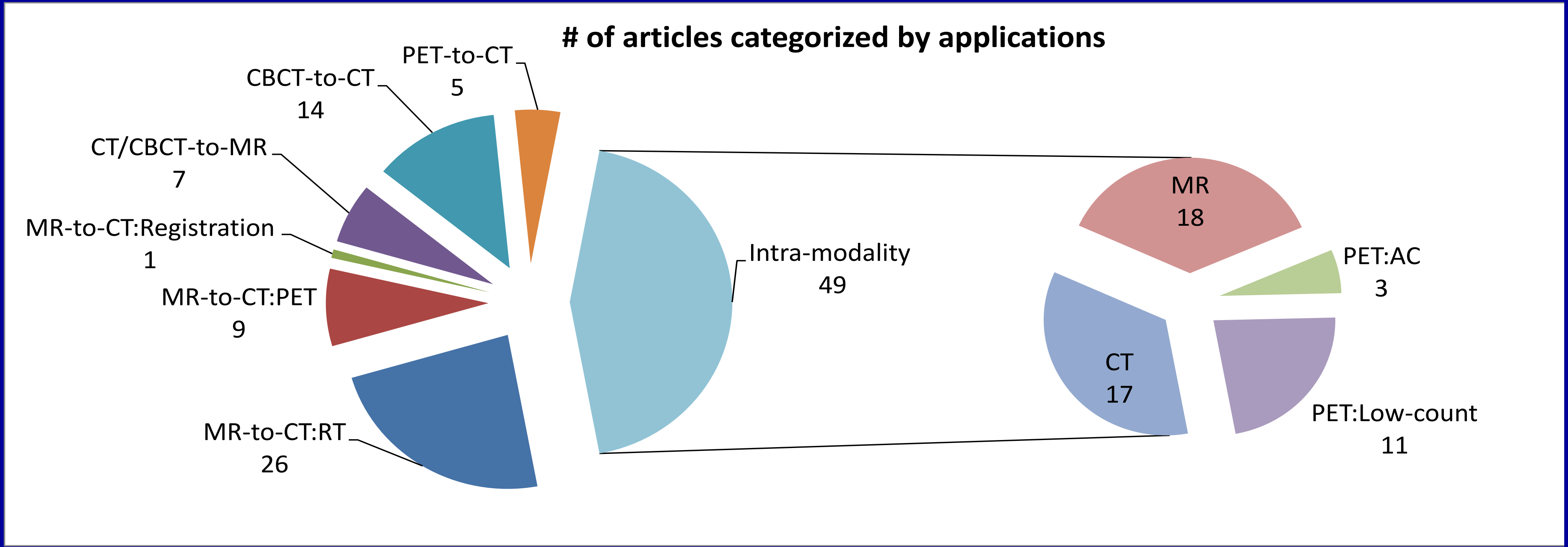

Wang T, … Yang X*, "Medical Imaging Synthesis using Deep Learning and its Clinical Applications: A Review," arXiv:2004.10322, 2020

Outline

- **Inter-modality**
  - MRI-based synthetic CT
  - CBCT-based synthetic CT
  - CBCT/CT-based synthetic MRI
  - PET-based synthetic CT
- **Intra-modality**
  - Low-quality to high-quality image synthesis
    - Non-AC to AC PET
    - Low-to-high dose PET or CT
    - Low-to-high resolution imaging
    - 2D-3D generation
  - Cross-sequence MRI synthesis
  - SECT-based synthetic DECT
  - CBCT-based relative stopping power map

MRI-based Synthetic CT

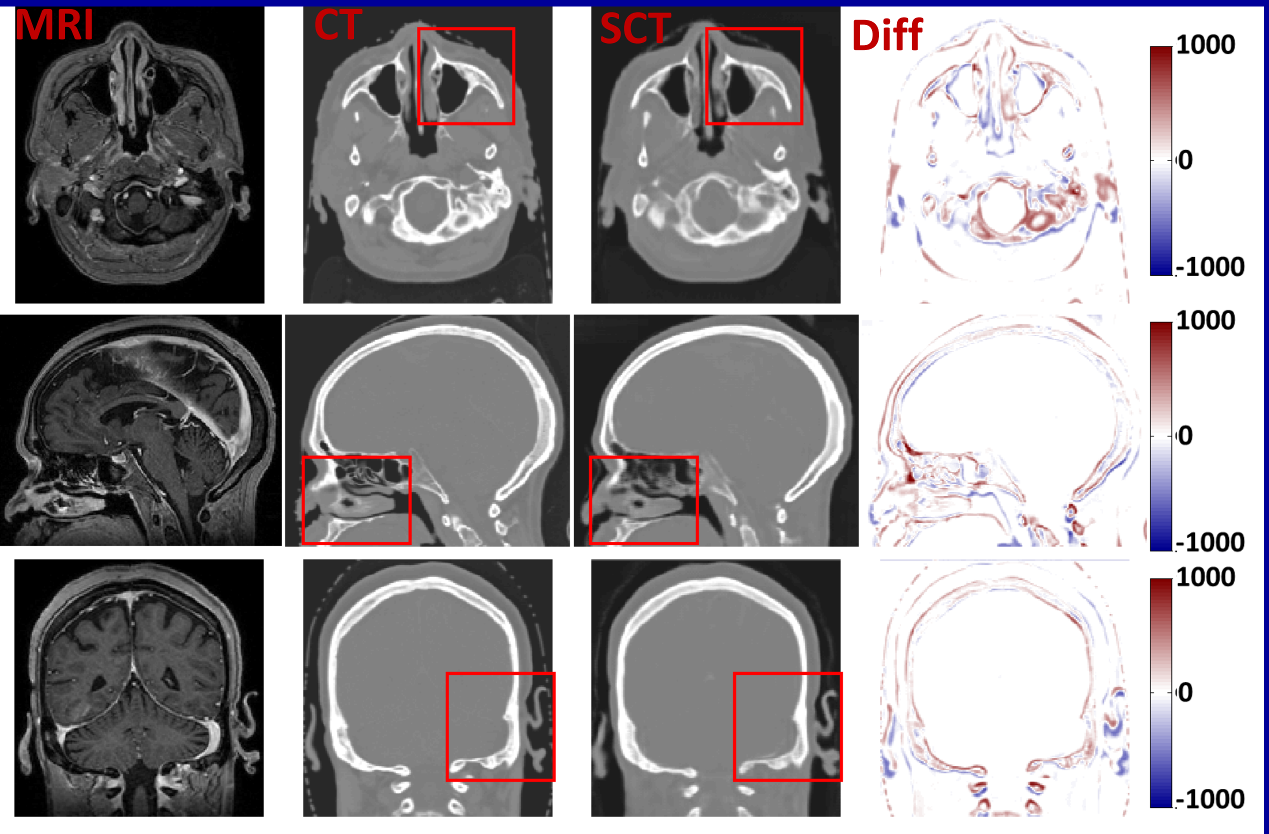

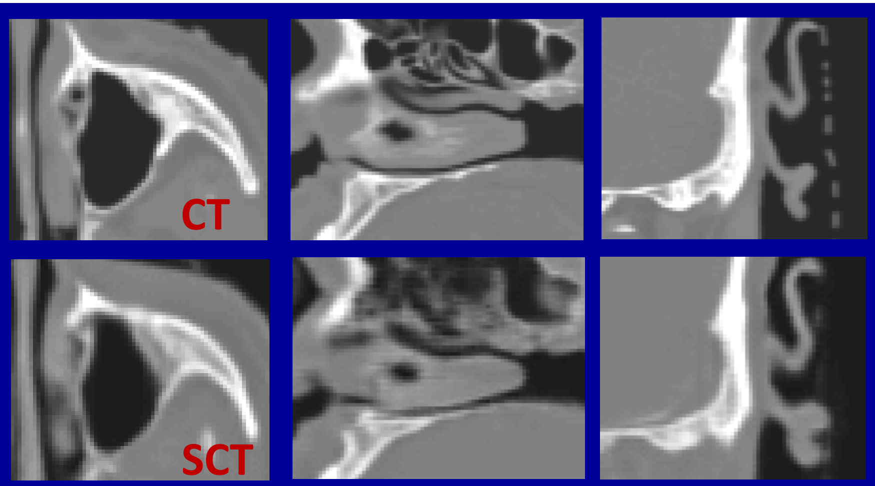

Yang X, … Liu T. *Proc of SPIE,* 101332Q, 2017

Lei Y, … Yang X. *JMI,* 5 (3), 034001, 2018

Lei Y, … Yang X. *JMI,* 5 (4), 043504, 2018

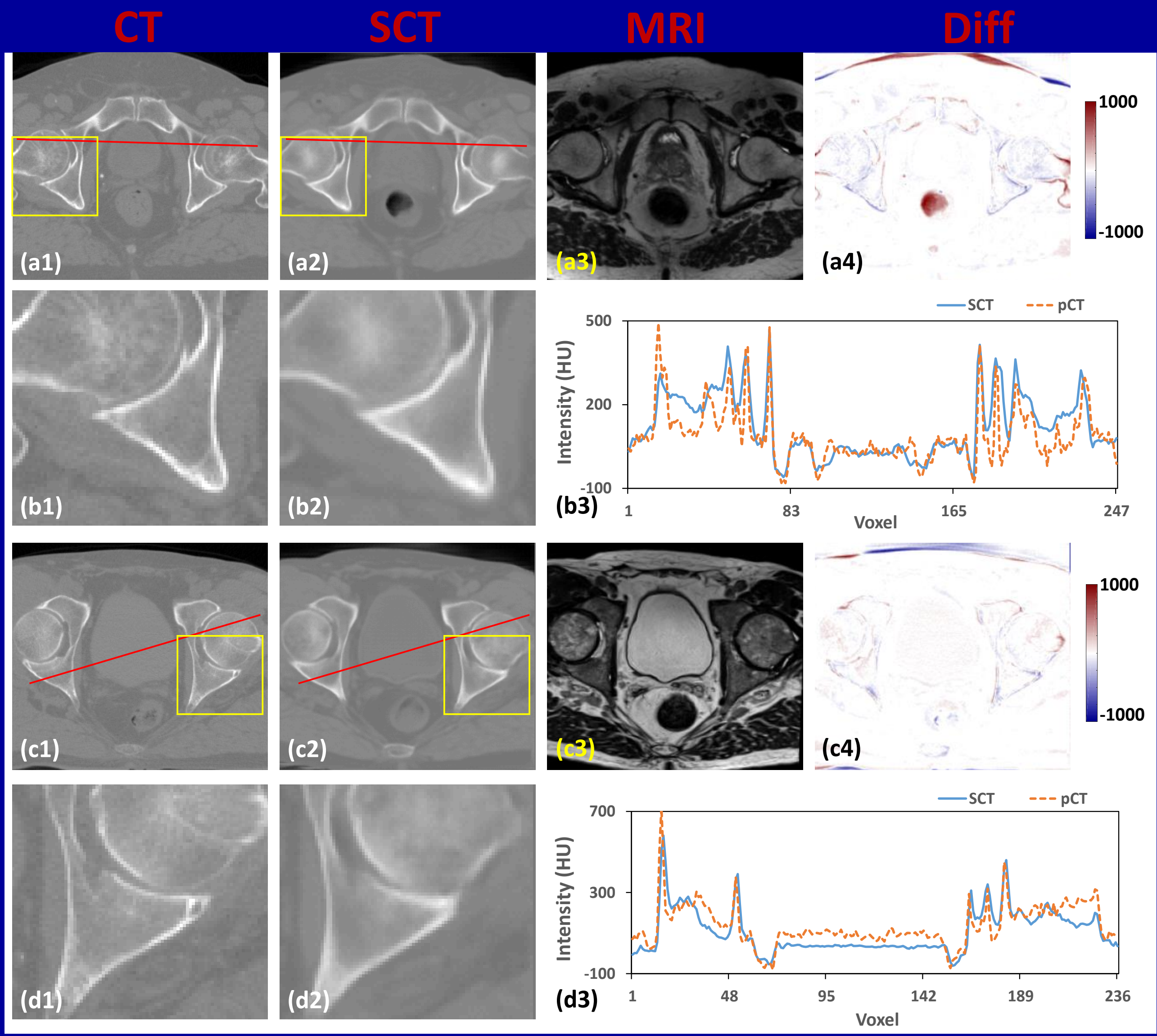

Liu Y, … Yang X. *PMB,* 64(14), 145015, 2019.

Wang T, … Yang X. *Medical Dosimetry,* 18, 30088-8, 2018.

Shafai G, … Yang X. *IJPT, 6*(2), 12-25, 2019.

Lei Y, … Yang X. *PMB,* 64 (8), 085001, 2019

Liu Y, … Yang X. *PMB, 64(20), 205022, 2019.*

Lei Y, … Yang X. *Med. Phy.,* 46(8), 3565-3581, 2019

MRI-based Synthetic CT for Emory Proton Center (First Case)

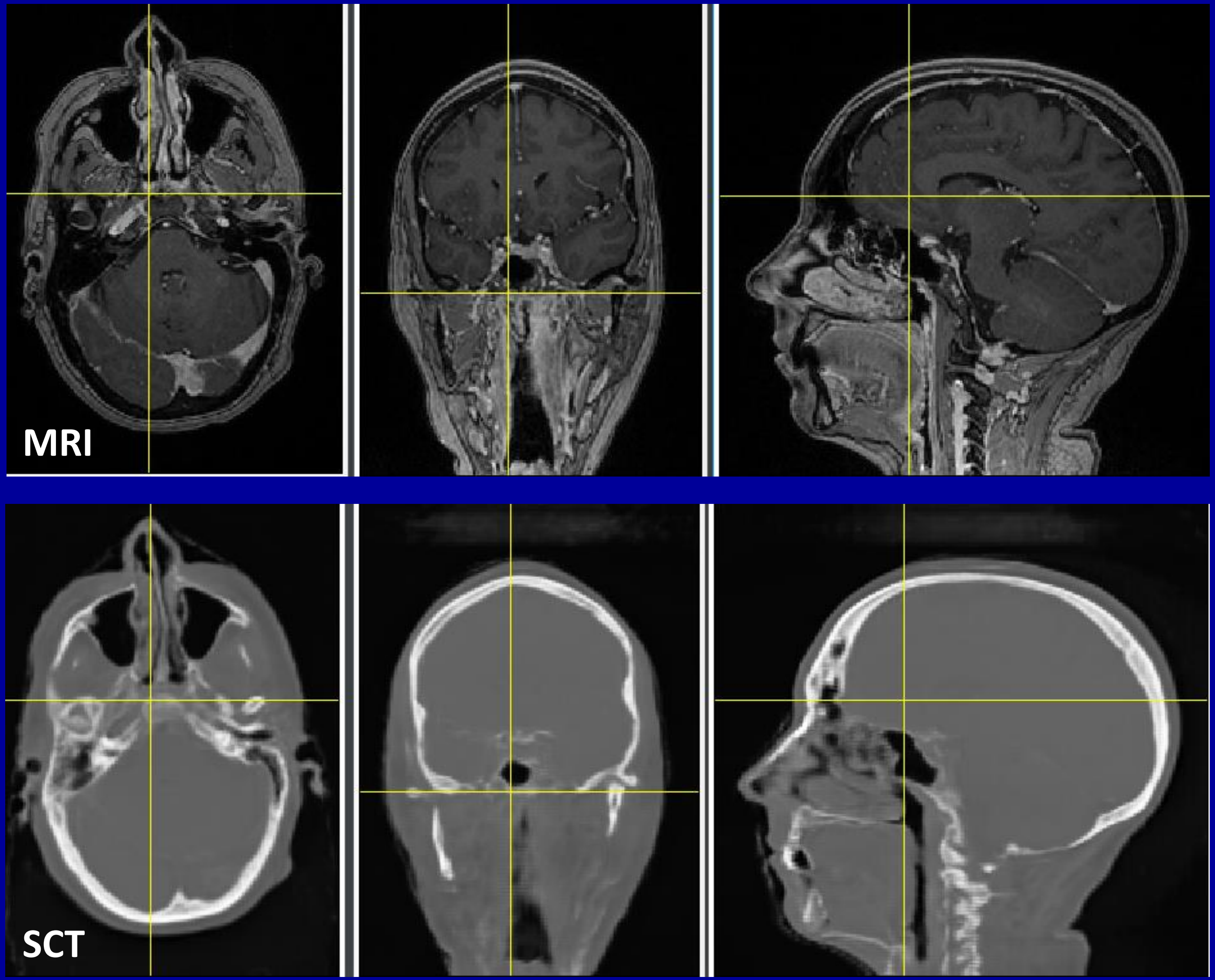

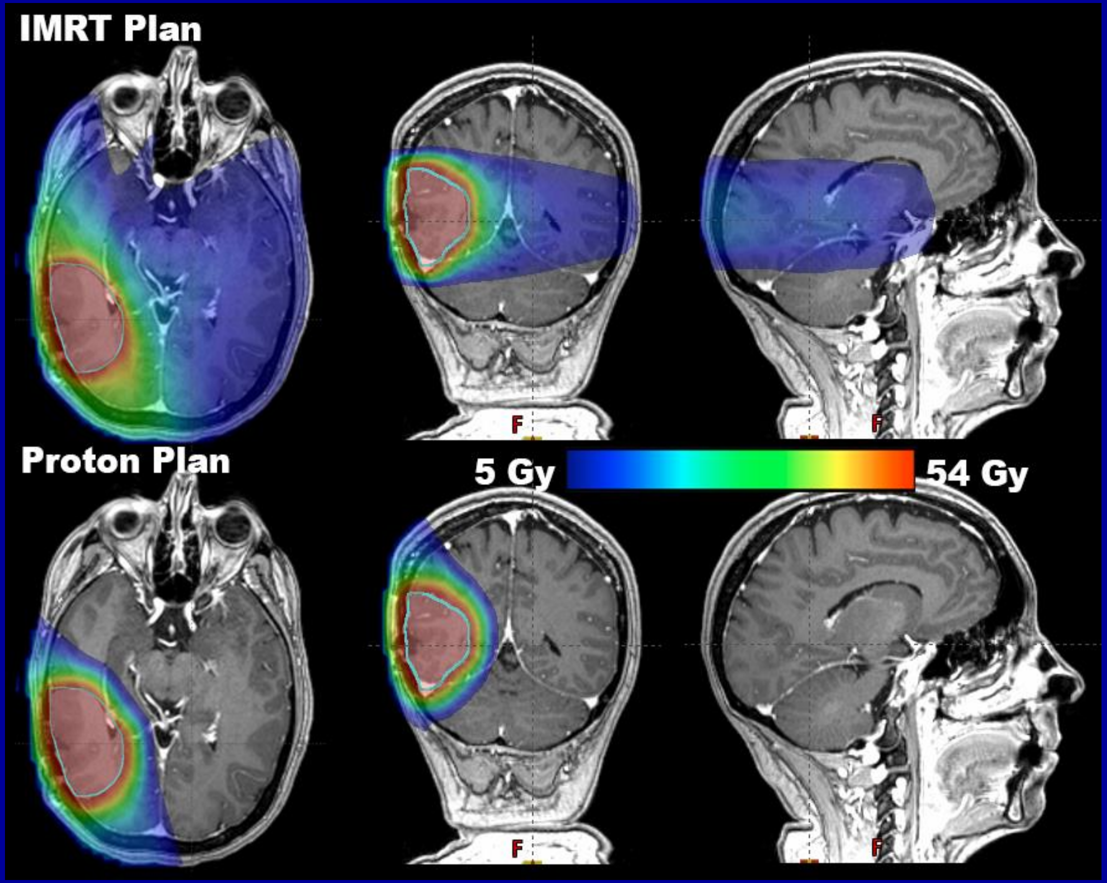

- 32 patients (2 cases per month)
  - Brain
  - Head and neck
  - Abdomen
  - Pelvis

Synthetic CT-aided MRI-CT Registration

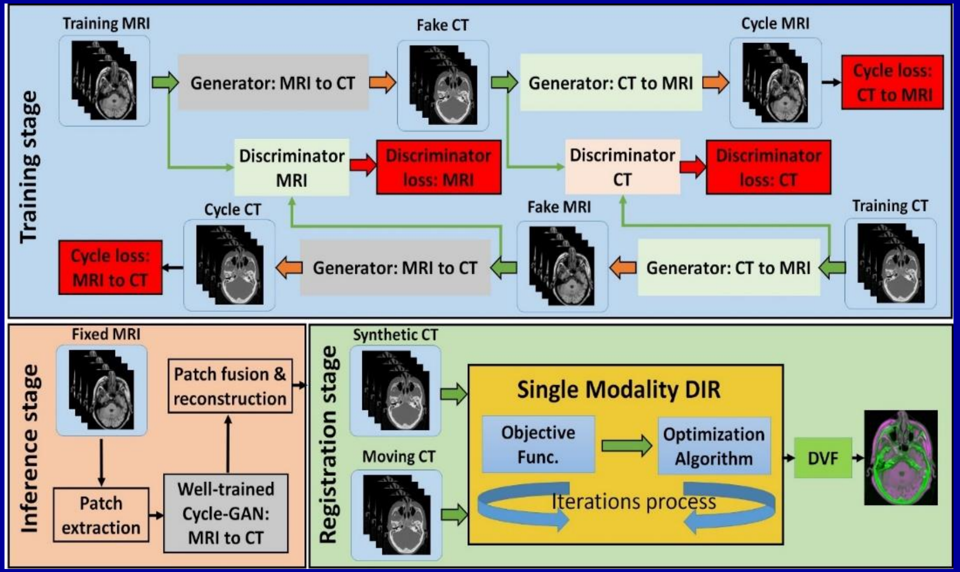

	TRE (mm)		NCC
Patient	CT-MRI	**CT-sCT**	CT-sCT
1	1.38	**1.11**	0.97
2	1.47	**1.26**	0.98
3	0.71	**0.67**	0.97
4	1.15	**1.12**	0.97
5	1.86	**0.93**	0.96
Mean	1.31	**1.02**	0.97

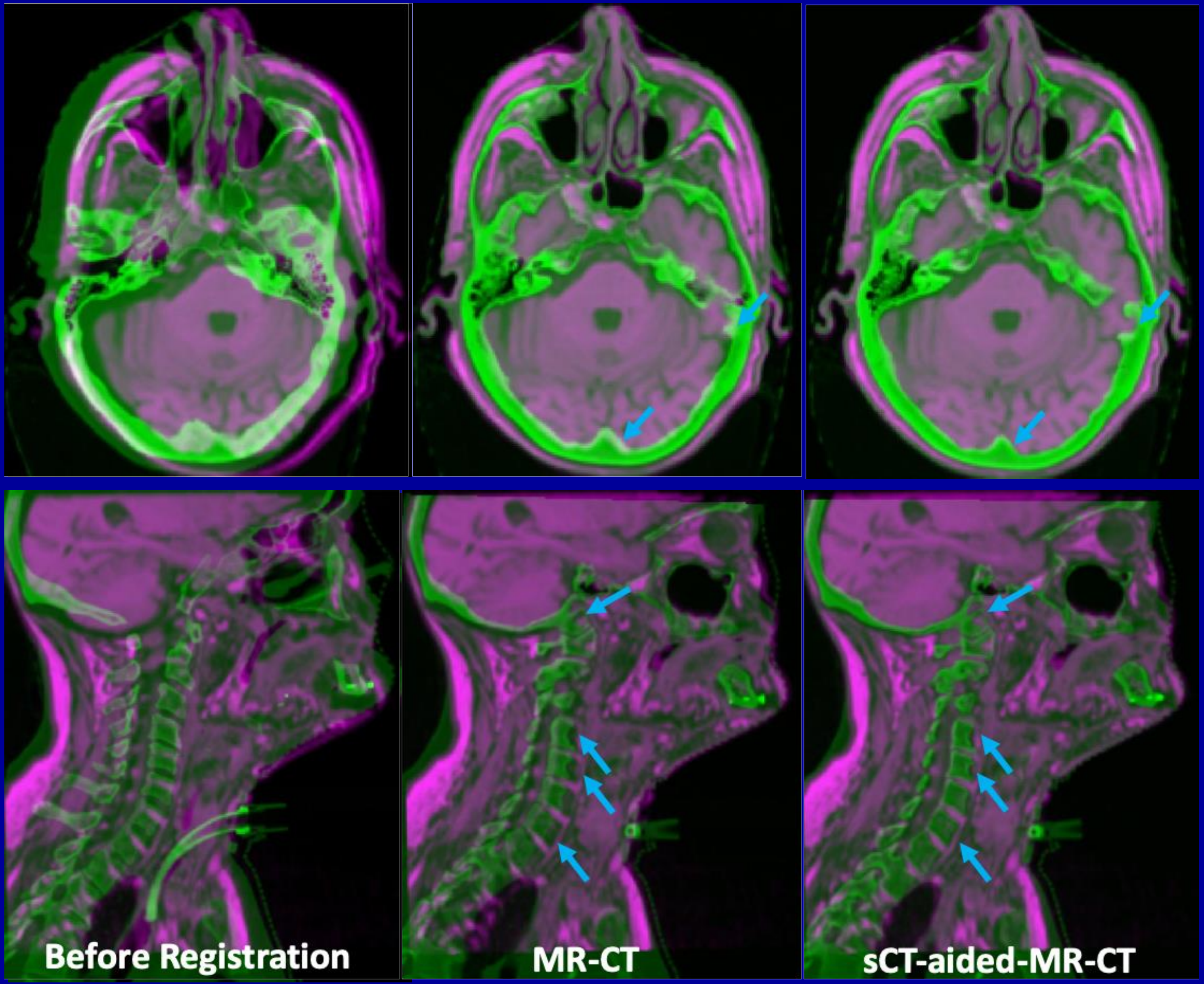

Fu Y, … Yang X. *Proc of SPIE,* 11313, 1131329, 2020.

MRI-based Synthetic CT for PET Attenuation Correction (AC)

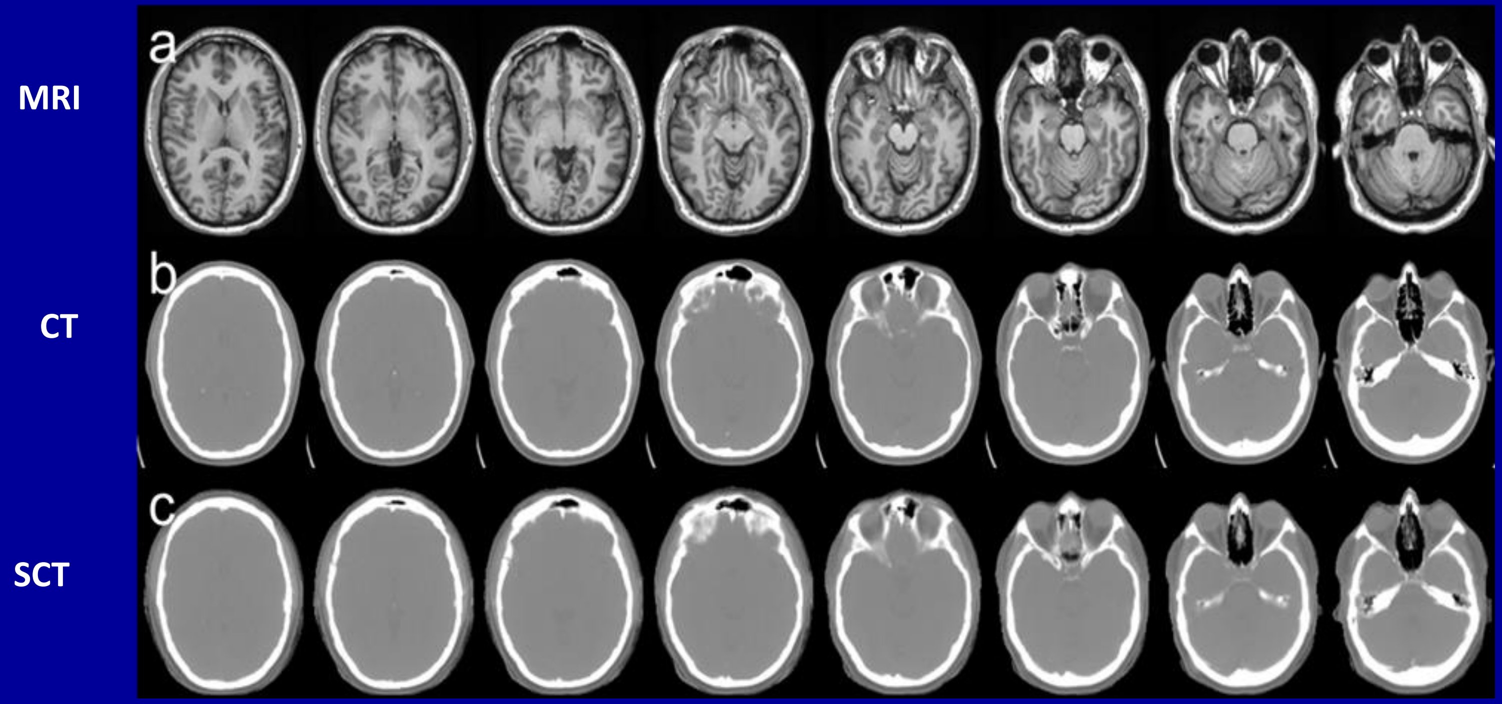

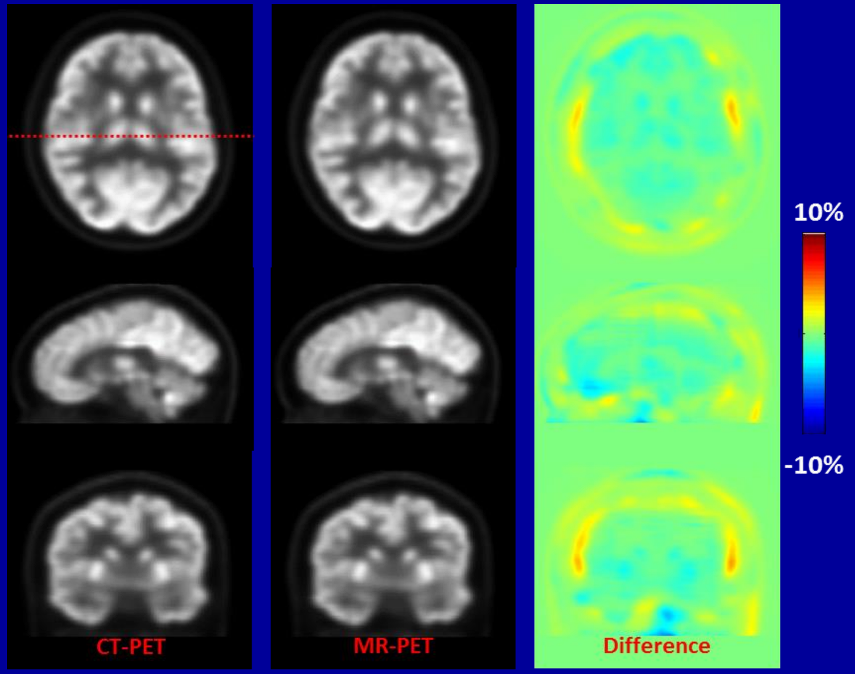

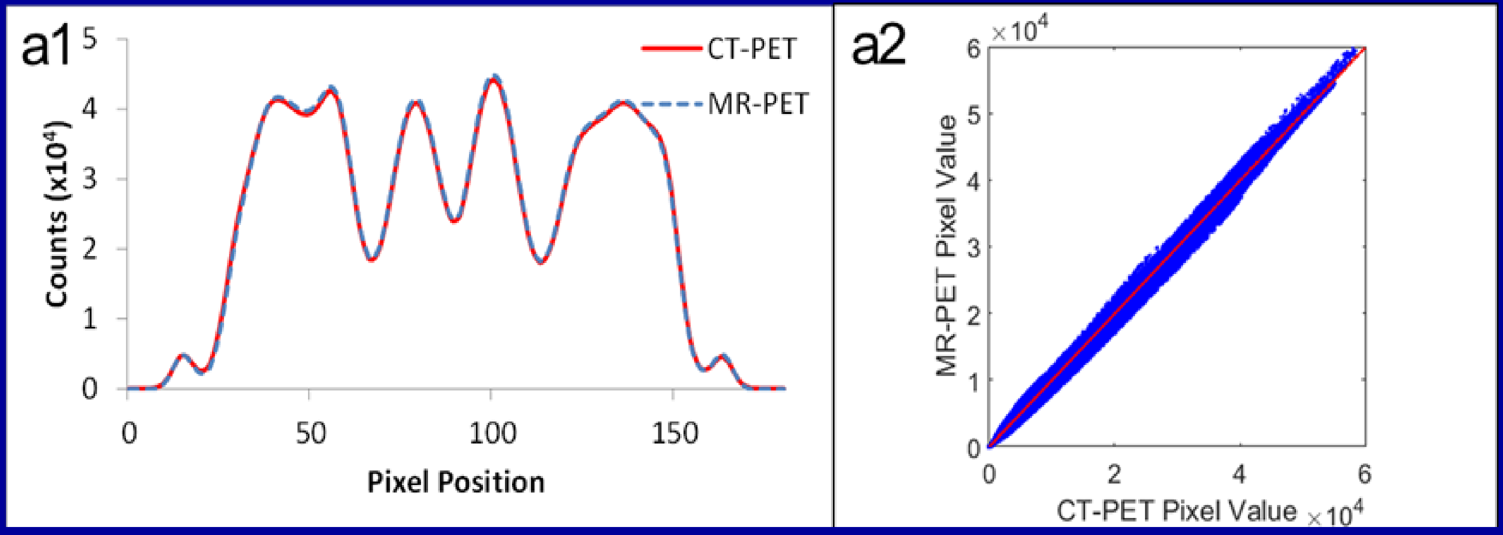

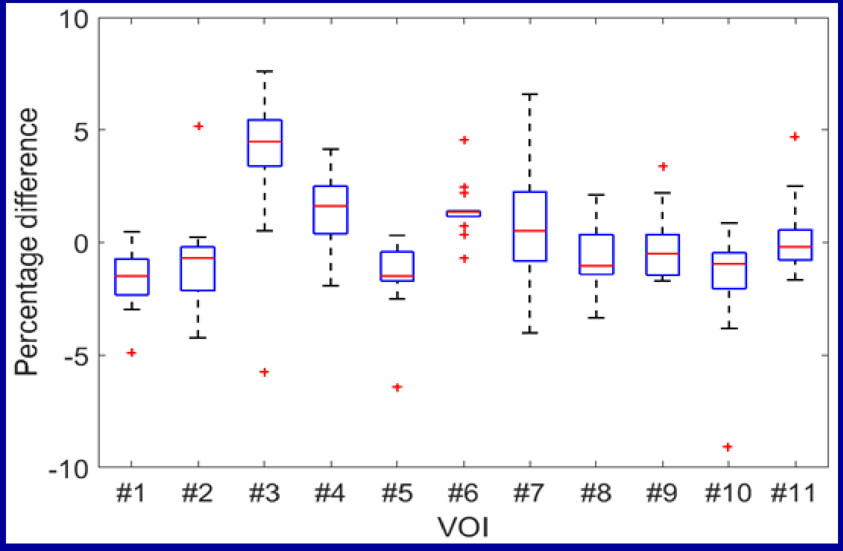

Fei B, Yang X ...Votaw J. *Med. Phy.*, 39(10), 2012 Yang X ...Fei B. *JAMIA*, 20(6), 2013 Yang X ... Jonathan N. *PMB*, 64(2), 2019 Lei Y ... Yang X. *PMB*, 64(8), 2019

Outline

- **Inter-modality**
  - MRI-based synthetic CT
  - CBCT-based synthetic CT
  - CBCT/CT-based synthetic MRI
  - PET-based synthetic CT
- **Intra-modality**
  - Low-quality to high-quality image synthesis
    - Non-AC to AC PET
    - Low-to-high dose PET or CT
    - Low-to-high resolution imaging
    - 2D-3D generation
  - Cross-sequence MRI synthesis
  - SECT-based synthetic DECT
  - CBCT-based relative stopping power map

CBCT-based Synthetic CT

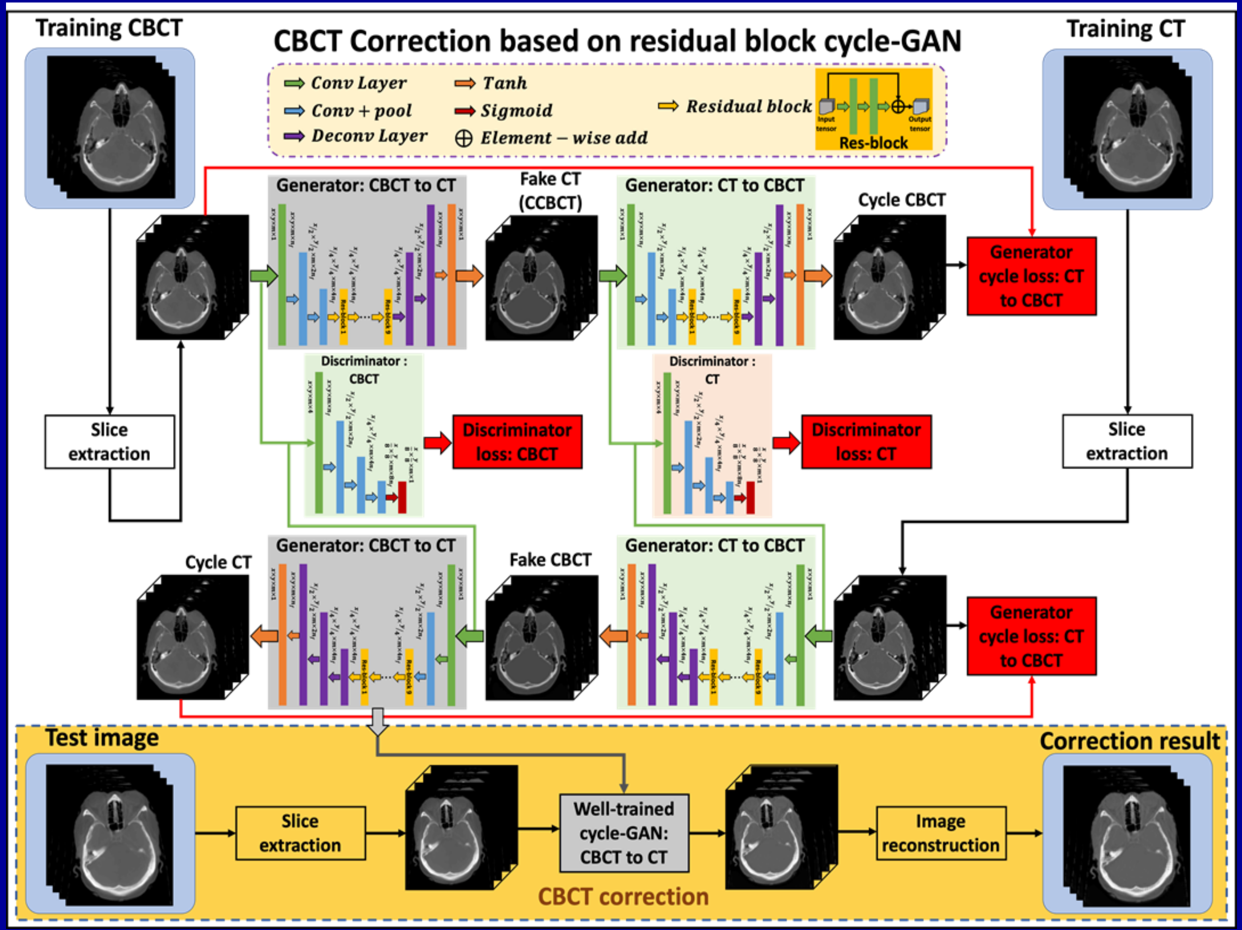

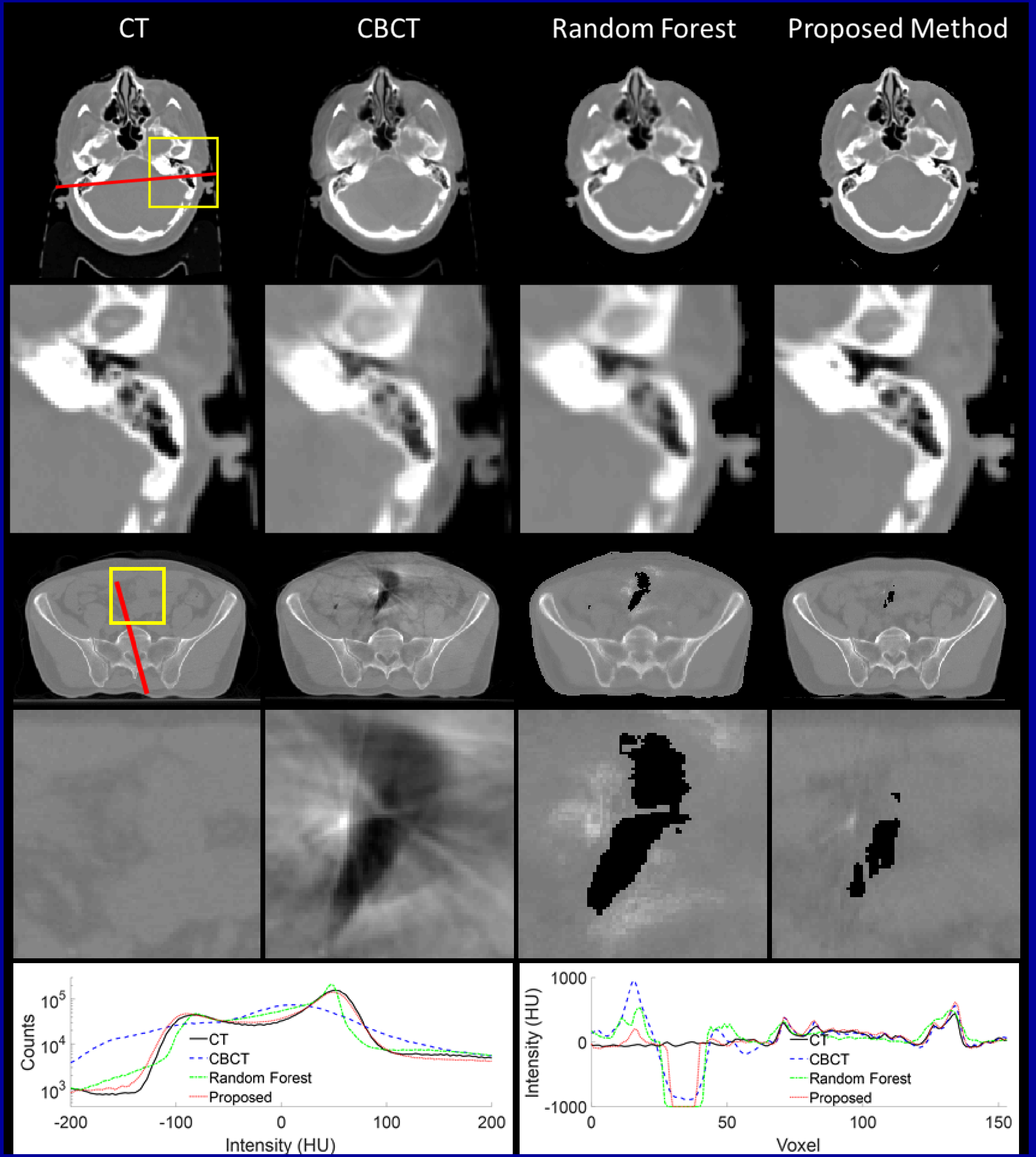

Lei Y, … Yang X. *Medical Physics,* 46(2), 601-618, 2019.

Harms J, … Yang X. *Medical Physics,* 46(9), 3998-4009, 2019.

CBCT-Guided Adaptive Photon and Proton Radiotherapy

Photon

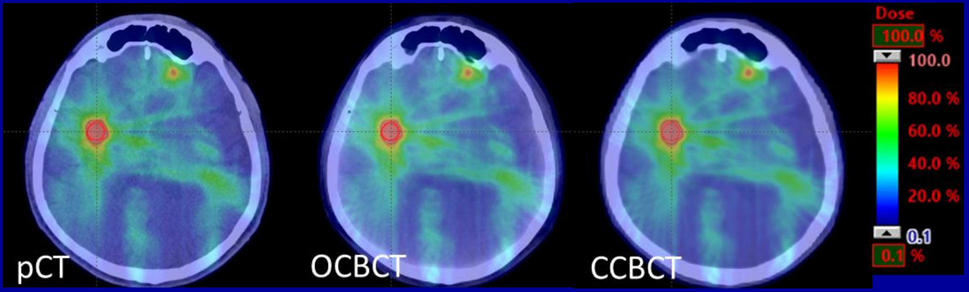

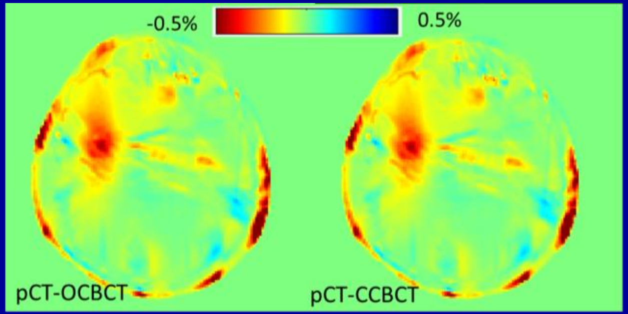

Proton

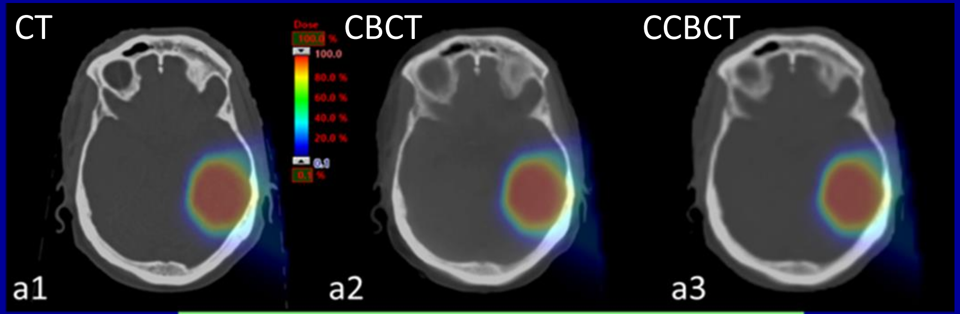

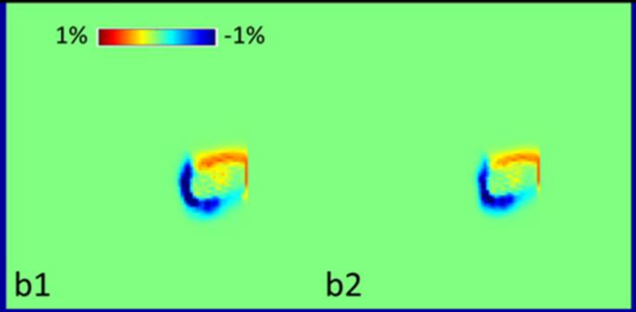

Photon

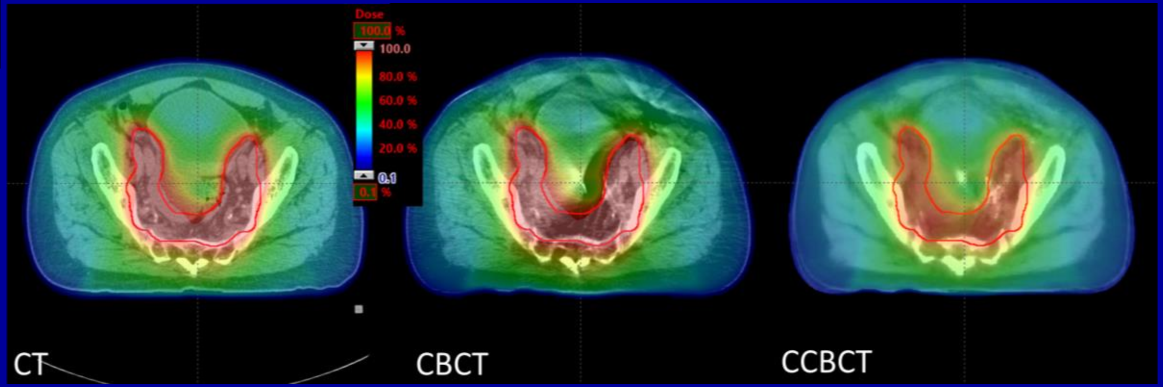

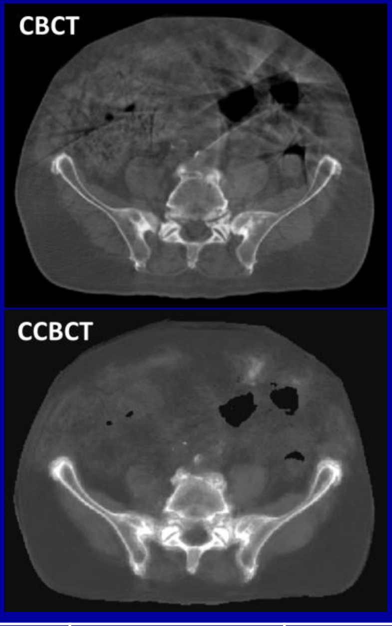

50 pts	Before Correction	After Correction (SCT)
MAE (HU)	56.3±19.7	16.1±4.5

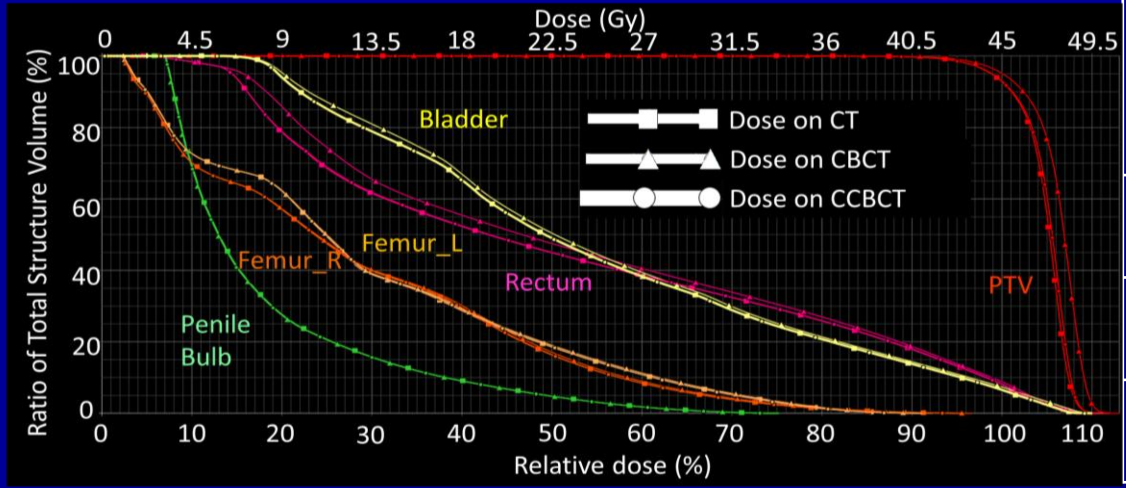

PTV (37 Plans)	Dose Diff [CBCT-CT /CCBCT-CT] (%)	P-Value
D_{50}	0.67±0.64/ 0.04±0.38	<0.01
D_{max}	1.33±1.46/ 0.46±1.02	0.03
D_{mean}	0.68±0.64/ 0.05±0.38	<0.01

Liu Y, … Yang X. *Med. Phy.*, 2020 (In press).

Wang T, … Yang X. *Medical Dosimetry, 44(3), 2019.*

Synthetic CT-aided CBCT-CT Registration

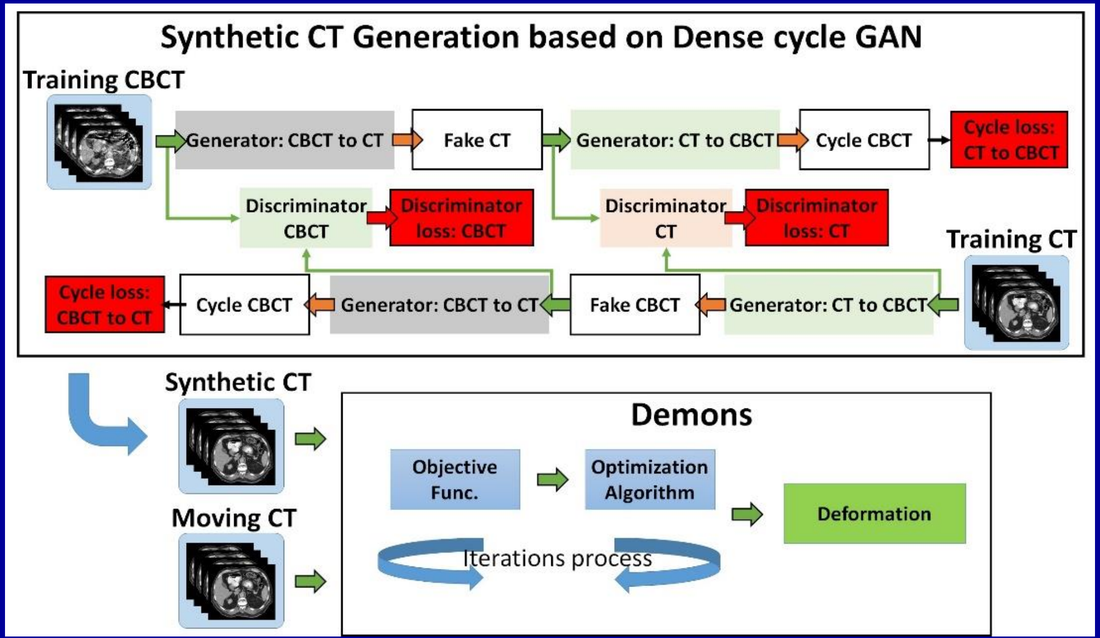

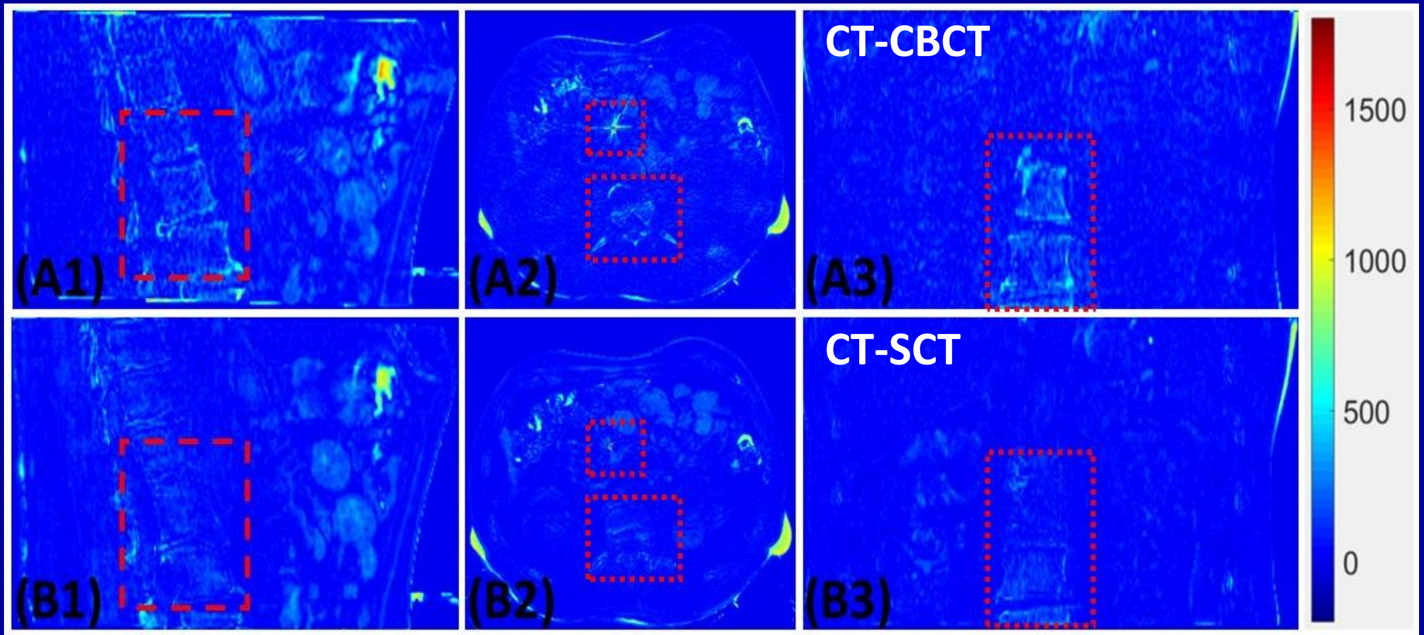

Fu Y… Yang X. *Proc of SPIE,* 11313, 113132U, 2020.

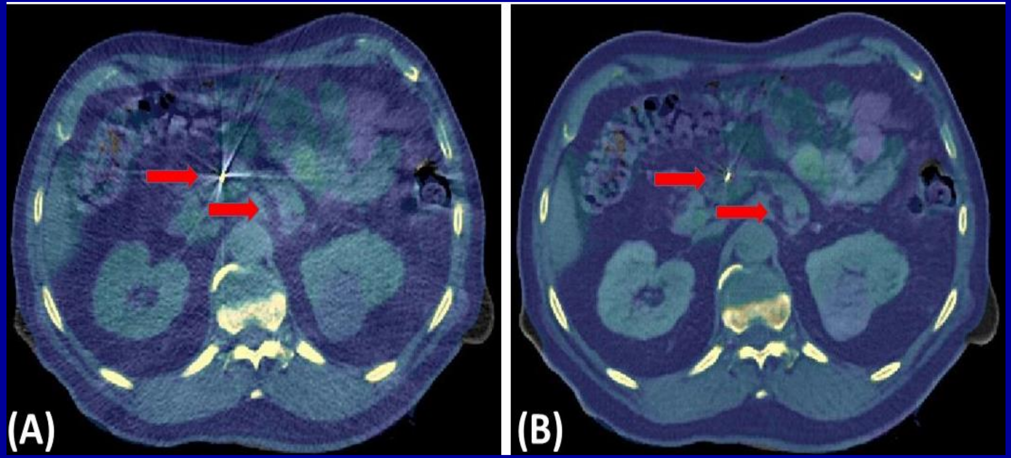

CBCT-CT SCT-CT

Outline

- **Inter-modality**
  - MRI-based synthetic CT
  - CBCT-based synthetic CT
  - CBCT/CT-based synthetic MRI
  - PET-based synthetic CT
- **Intra-modality**
  - Low-quality to high-quality image synthesis
    - Non-AC to AC PET
    - Low-to-high dose PET or CT
    - Low-to-high resolution imaging
    - 2D-3D generation
  - Cross-sequence MRI synthesis
  - SECT-based synthetic DECT
  - CBCT-based relative stopping power map

Multiple Organ Segmentation in Head and Neck CT Aided by sMRI

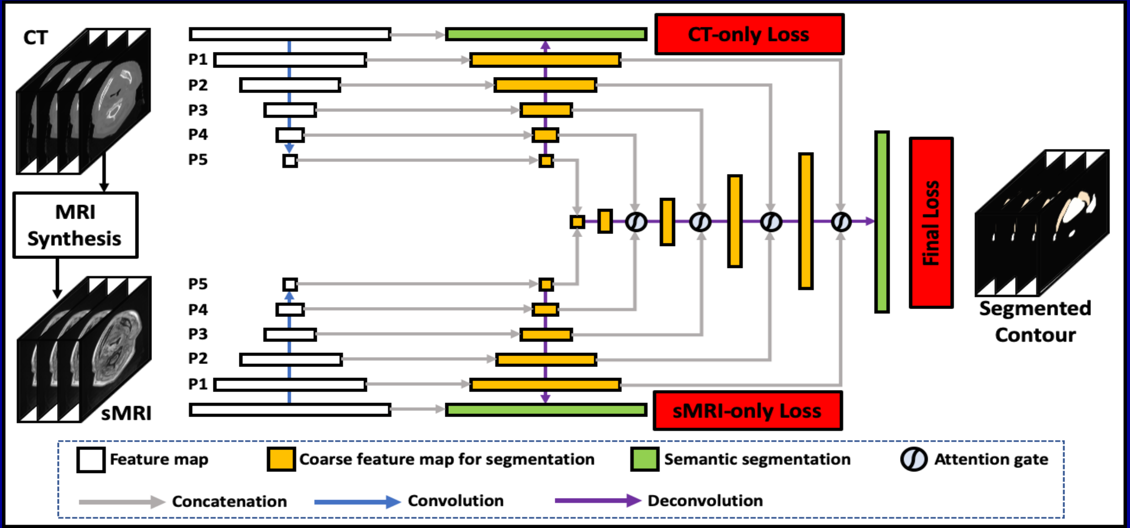

Liu Y… Yang X, *Medical Physics*, 2020 (Accepted)

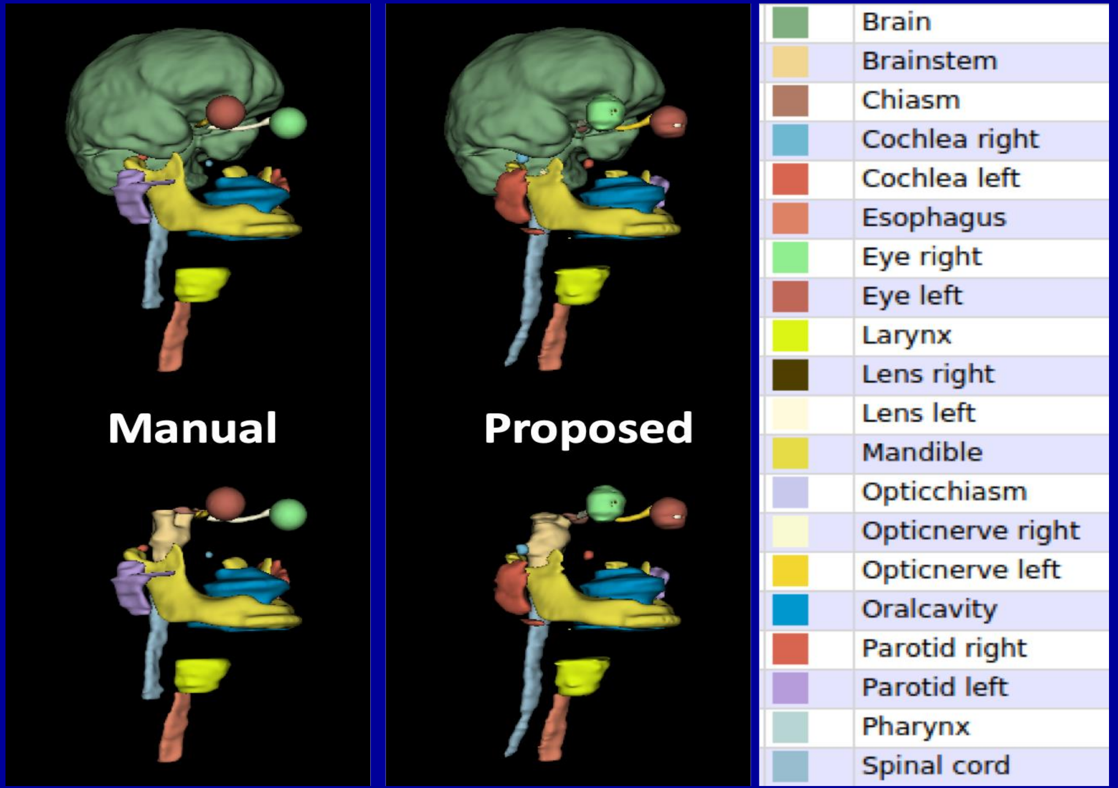

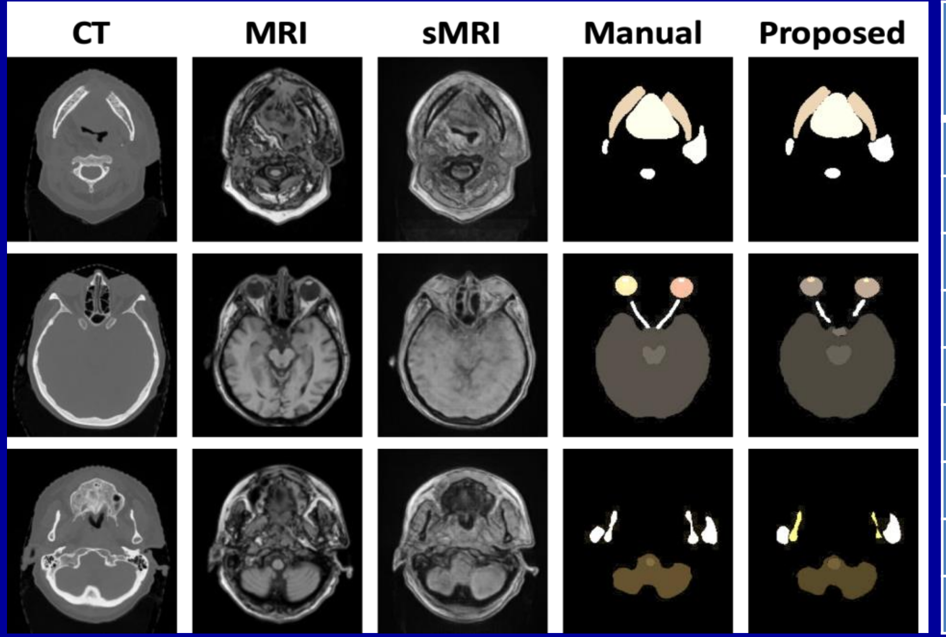

PDDCA Challenge Data (Dice)	Wang *et al.* 2019	Tong *et al.* 2018	Tang *et al.* 2019	Zhu *et al.* 2018	Our
Brain Stem	0.88 ± 0.02	0.87 ± 0.03	0.87 ± 0.03	0.87 ± 0.02	**0.91 ± 0.02**
Chiasm	0.45 ± 0.17	0.58 ± 0.1	0.62 ± 0.1	0.53 ± 0.15	**0.73 ± 0.11**
Mandible	0.93 ± 0.02	0.87 ± 0.03	0.95 ± 0.01	0.93 ± 0.02	**0.96 ± 0.01**
OpticNerve_L	0.74 ± 0.15	0.65 ± 0.05	0.75 ± 0.07	0.72 ± 0.06	**0.78 ± 0.09**
OpticNerve_R	0.74 ± 0.09	0.69 ± .0.5	0.72 ± 0.06	0.71 ± 0.1	**0.78 ± 0.11**
Parotid_L	0.86 ± 0.02	0.84 ± 0.02	**0.89 ± 0.02**	0.88 ± 0.02	0.88 ± 0.04
Parotid_R	0.85 ± 0.07	0.83 ± 0.02	**0.88 ± 0.05**	0.87 ± 0.04	**0.88 ± 0.06**
Submandibular_L	0.76 ± 0.15	0.76 ± 0.06	0.82 ± 0.05	0.81 ± 0.04	**0.86 ± 0.08**
Submandibular_R	0.73 ± 0.01	0.81 ± 0.06	0.82 ± 0.05	0.81 ± 0.04	**0.85 ± 0.10**

Multiple OAR Segmentation in Pelvic CBCT Aided by sMRI

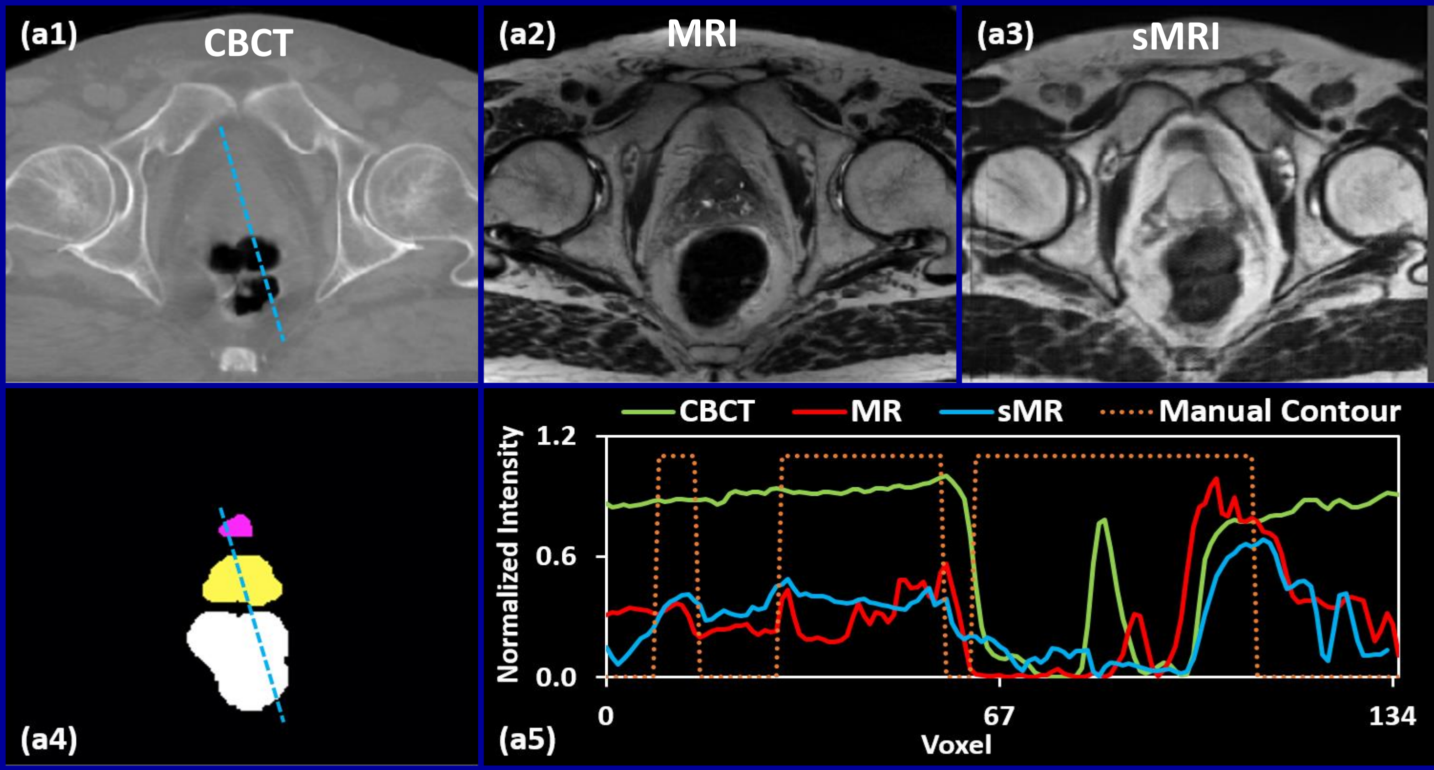

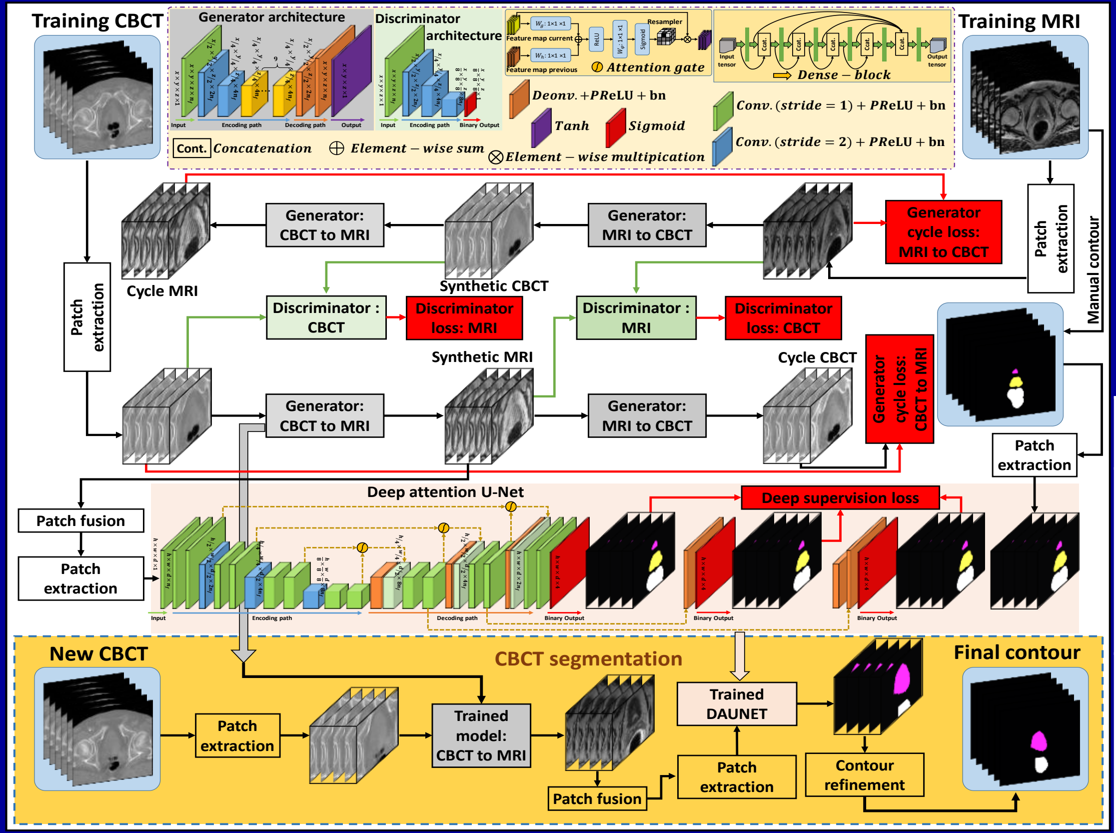

	Method	DSC	HD (mm)	MSD (mm)	RMSD (mm)	CMD (mm)	VD (cc)
Bladder	DSUNet sMRI	0.93±0.05	6.45±5.24	0.51±0.27	0.81±0.52	1.29±1.28	8.642±7.23
	DAUNet CBCT	0.90±0.06	11.32±12.75	0.74±0.44	1.18±0.76	2.08±2.29	14.26±16.59
	DAUNet sMRI	0.95±0.02	4.69±4.92	0.44±0.22	0.80±0.69	0.90±0.68	6.55±6.68
	P-value (DAUNet sMRI vs. DSUNet sMRI)	0.003	0.049	0.154	0.960	0.023	0.096
	P-value (DAUNet sMRI vs. DAUNet CBCT)	<0.001	0.002	<0.001	0.009	<0.001	<0.001
Prostate	DSUNet sMRI	0.84±0.07	5.48±2.57	0.80±0.35	1.12±0.47	2.26±1.63	4.13±5.71
	DAUNet CBCT	0.82±0.09	5.83±3.30	0.9±0.47	1.30±0.66	2.58±1.92	3.98±5.21
	DAUNet sMRI	0.86±0.06	4.82±2.37	0.73±0.37	1.08±0.55	1.954±1.58	3.32±5.54
	P-value (DAUNet sMRI vs. DSUNet sMRI)	<0.001	0.043	0.126	0.584	0.179	0.317
	P-value (DAUNet sMRI vs. DAUNet CBCT)	<0.001	0.010	<0.001	0.009	0.031	0.403
Rectum	DSUNet sMRI	0.88±0.05	8.62±5.15	1.03±1.66	2.04±3.82	3.72±4.18	5.31±7.78
	DAUNet CBCT	0.83±0.07	13.14±18.71	1.19±0.87	2.31±2.51	3.92±4.65	8.32±8.47
	DAUNet sMRI	0.91±0.04	5.46±3.19	0.71±0.65	1.62±2.36	1.98±1.86	3.93±3.86
	P-value (DAUNet sMRI vs. DSUNet sMRI)	<0.001	<0.001	0.192	0.434	0.002	0.155
	P-value (DAUNet sMRI vs. DAUNet CBCT)	<0.001	0.006	0.001	0.130	0.005	<0.001

Workshop on Artificial Intelligence in Radiation Therapy
AIRT 2019: Artificial Intelligence in Radiation Therapy pp 154-161 | Cite as

CBCT-Based Synthetic MRI Generation for CBCT-Guided Adaptive Radiotherapy

Authors   Authors and affiliations

Yang Lei, Tonghe Wang, Joseph Harms, Yabo Fu, Xue Dong, Walter J. Curran, Tian Liu, Xiaofeng Yang

Physics in Medicine & Biology

ACCEPTED MANUSCRIPT

Male pelvic multi-organ segmentation aided by CBCT-based synthetic MRI

Yang Lei[1], Tonghe Wang[1], Sibo Tian[1], Xue Dong[2], Ashesh B Jani[1], David Schuster[3], Walter J Curran[4], Pretesh Patel[1], Tian Liu[5] and Xiaofeng Yang[1]

Accepted Manuscript online 18 December 2019 • © 2019 Institute of Physics and Engineering in Medicine

Non-AC PET-based Synthetic CT for PET Attenuation Correction (AC)

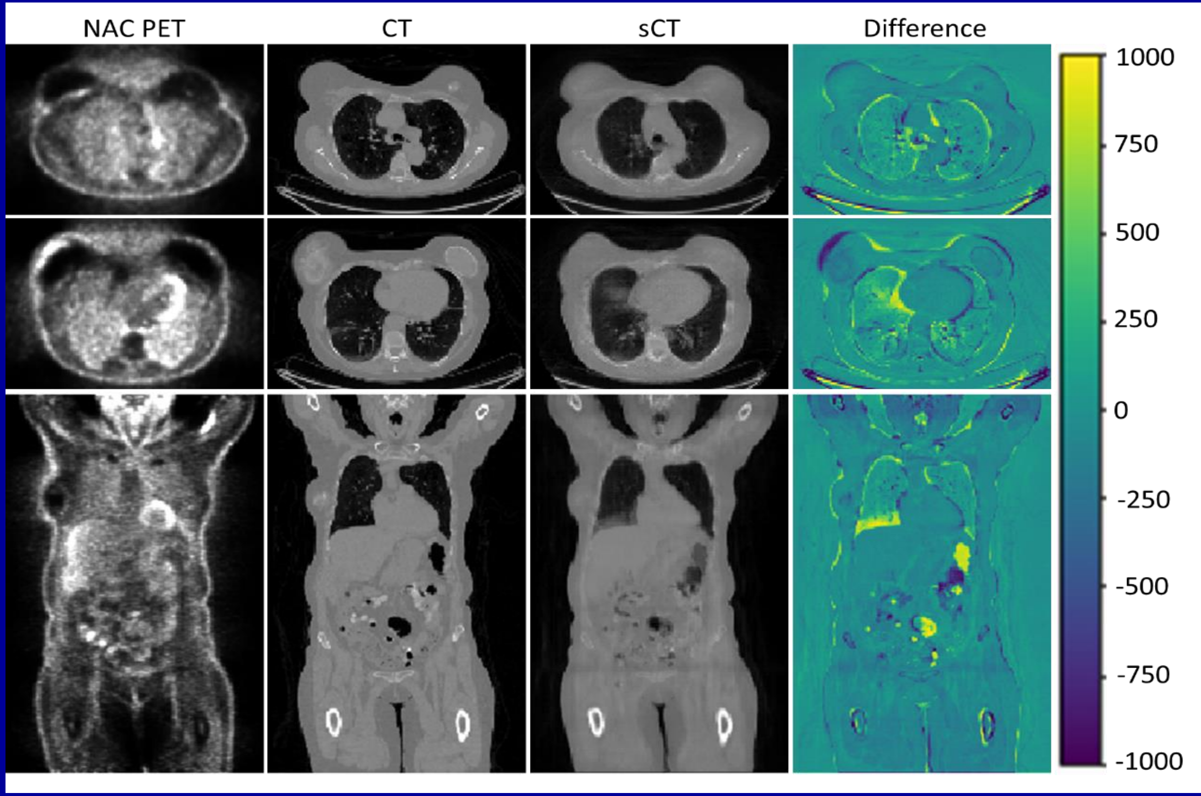

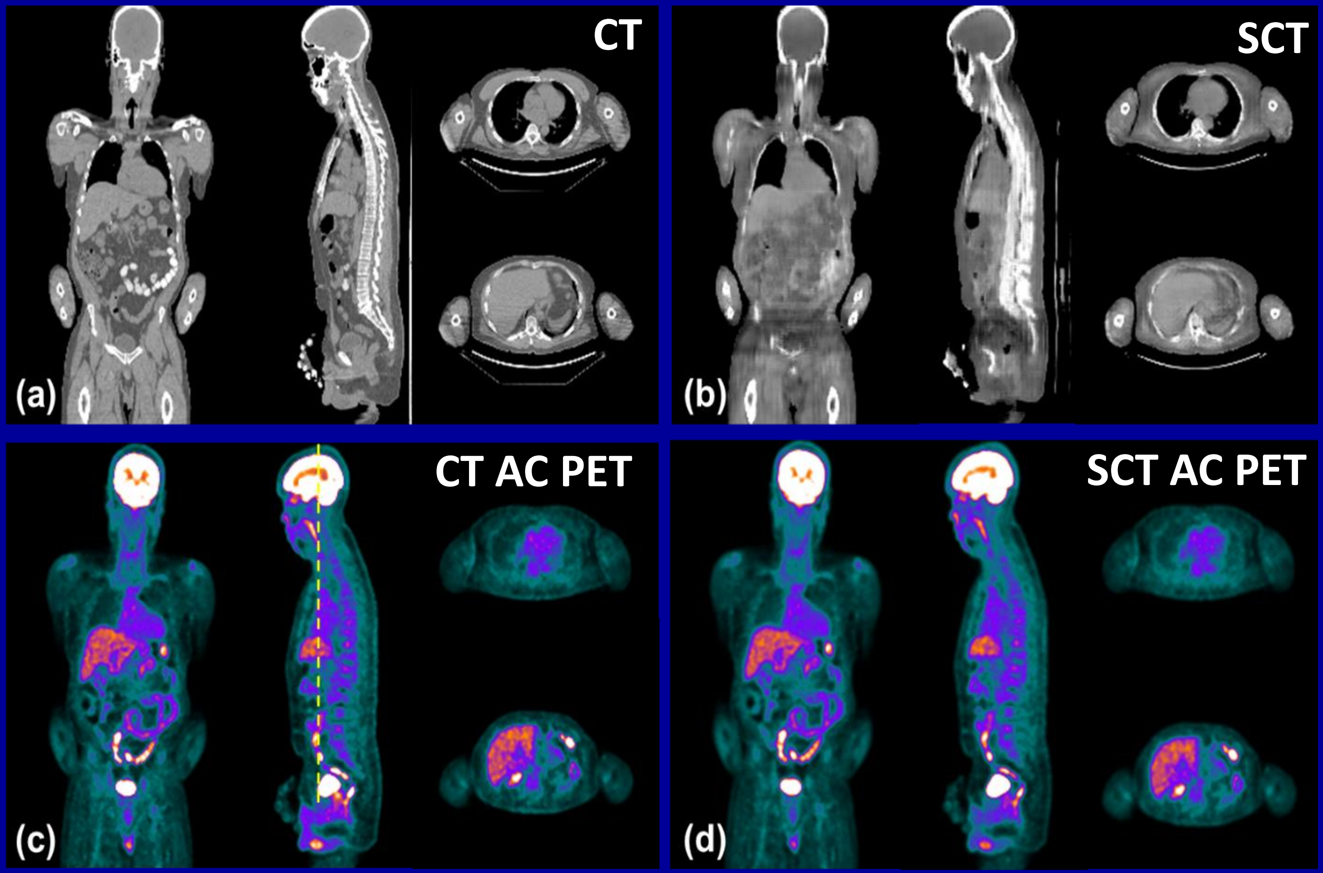

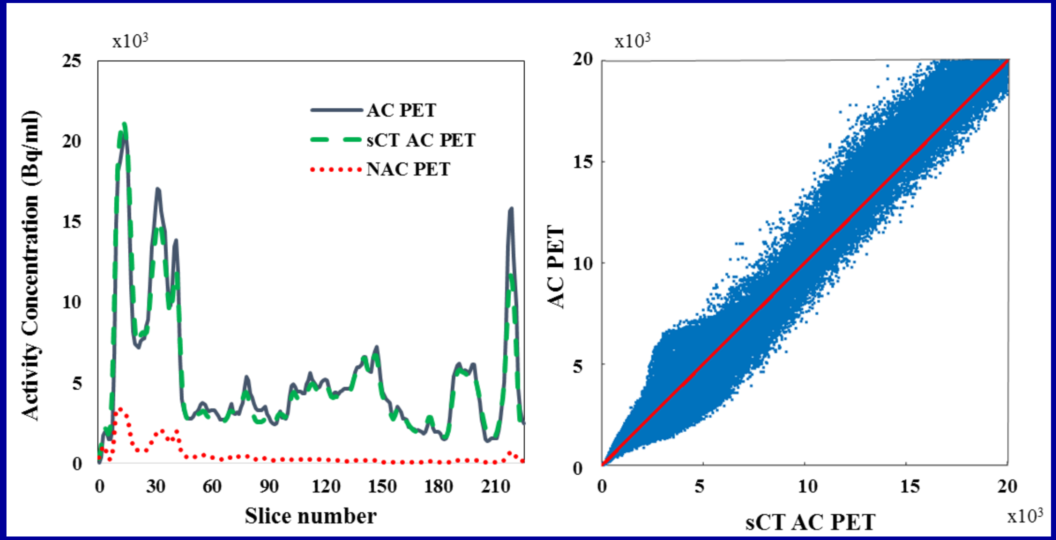

Physics in Medicine & Biology

PAPER

Synthetic CT generation from non-attenuation corrected PET images for whole-body PET imaging

Xue Dong[1,5], Tonghe Wang[1,5], Yang Lei[1], Kristin Higgins[1,2], Tian Liu[1,2], Walter J Curran[1,2], Hui Mao[2,3], Jonathon A Nye[3] and Xiaofeng Yang[1,4]

Published 4 November 2019 •

Outline

- **Inter-modality**
  - MRI-based synthetic CT
  - CBCT-based synthetic CT
  - CBCT/CT-based synthetic MRI
  - PET-based synthetic CT
- **Intra-modality**
  - Low-quality to high-quality image synthesis
    - Non-AC to AC PET
    - Low-to-high dose PET or CT
    - Low-to-high resolution imaging
    - 2D-3D generation
  - Cross-sequence MRI synthesis
  - SECT-based synthetic DECT
  - CBCT-based relative stopping power map

PET Self Attenuation Correction (AC)

Physics in Medicine & Biology

ACCEPTED MANUSCRIPT

Deep learning-based attenuation correction in the absence of structural information for whole-body PET imaging

Xue Dong[1], Yang Lei[1], Tonghe Wang[1], Kristin Higgins[2], Tian Liu[1], Walter J Curran[2], Hui Mao[3], Jonathon A Nye[4] and Xiaofeng Yang[1]

Accepted Manuscript online 23 December 2019 •

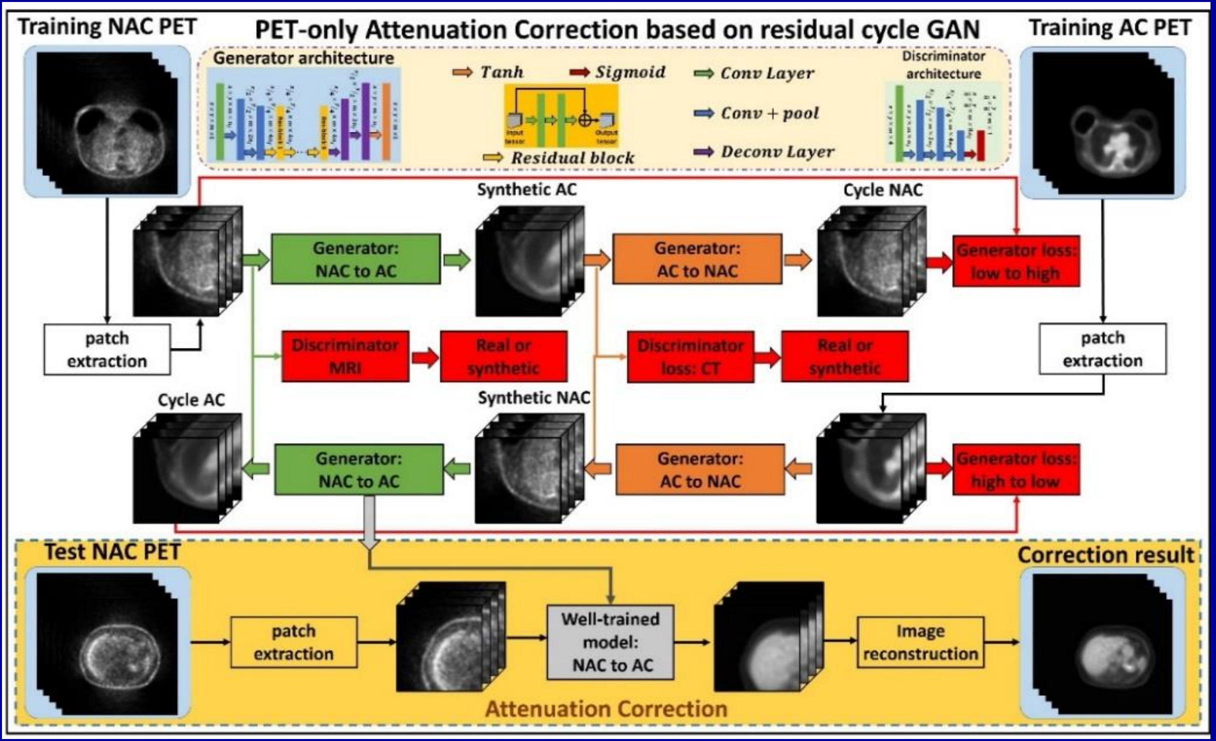

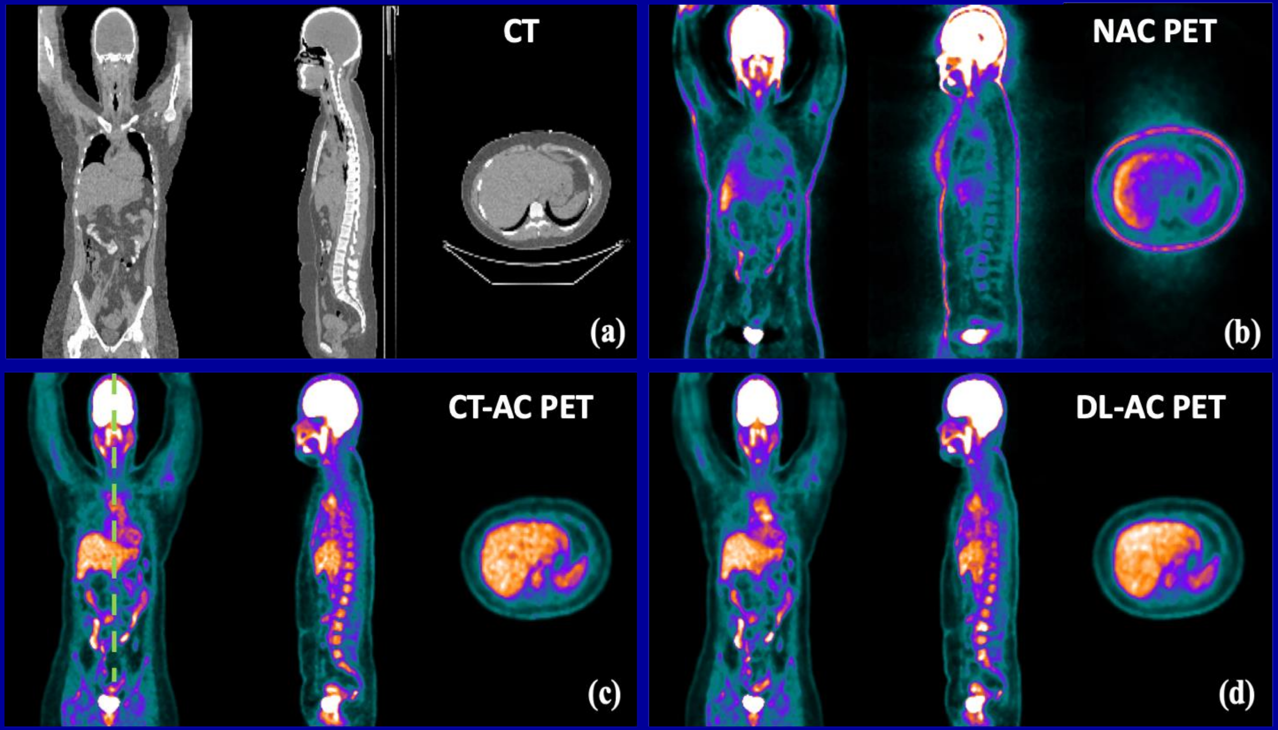

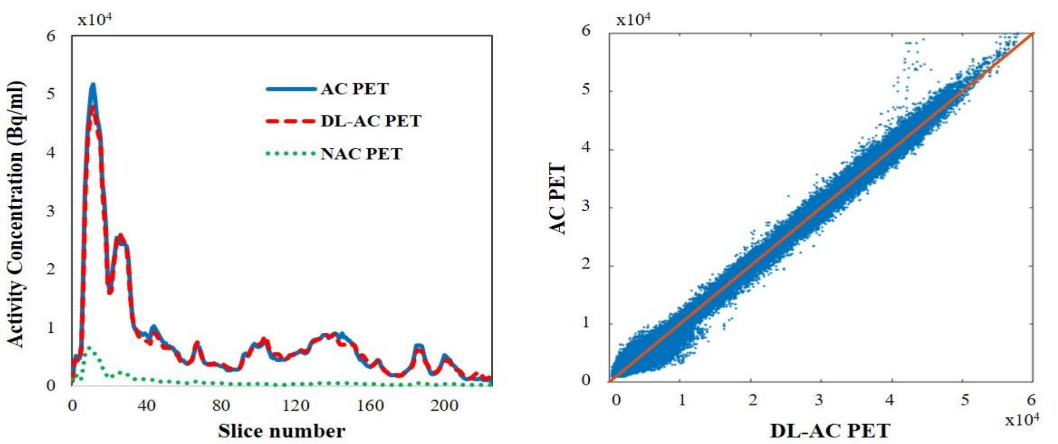

Low dose PET Imaging

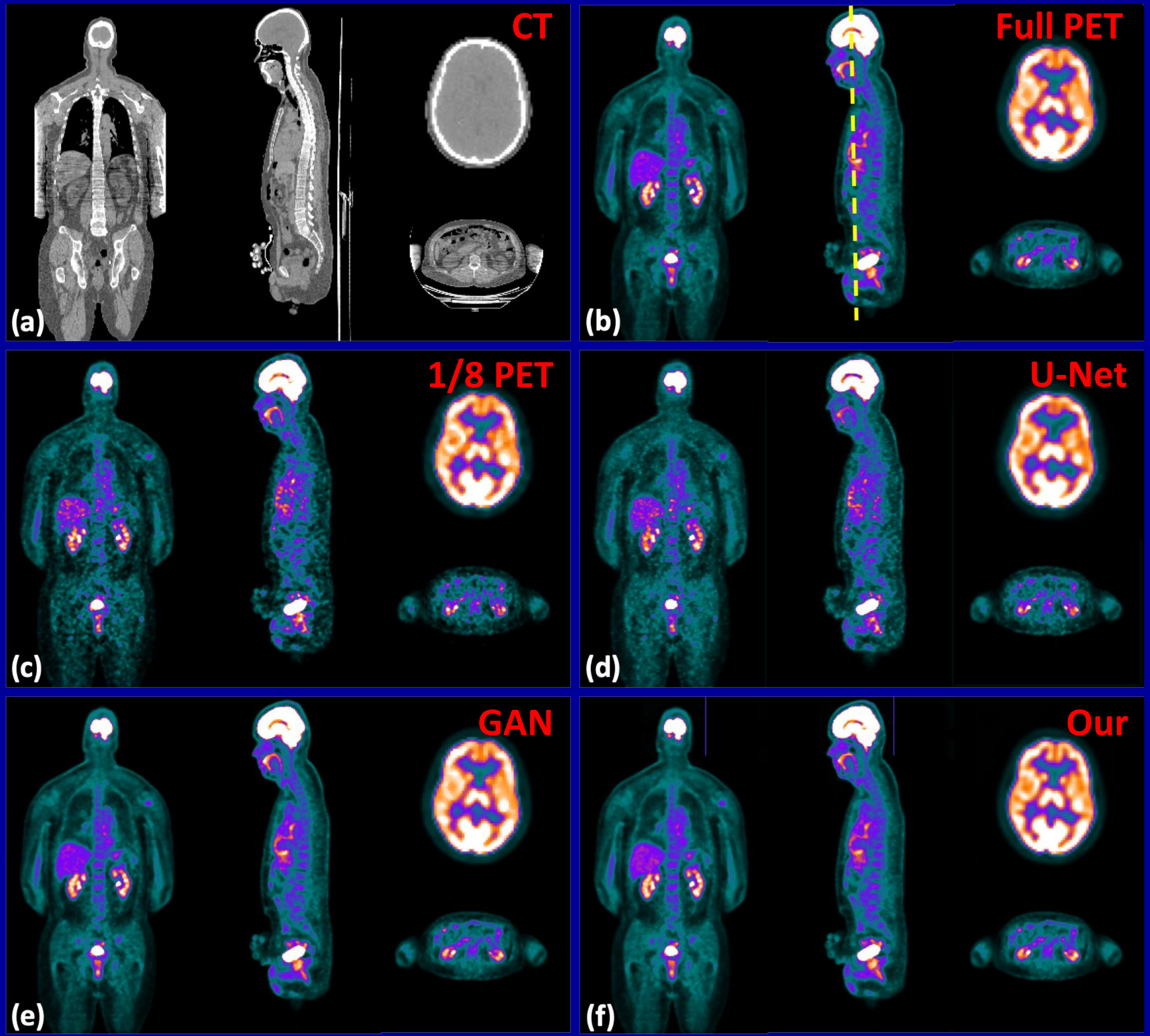

Physics in Medicine & Biology

PAPER

Whole-body PET estimation from low count statistics using cycle-consistent generative adversarial networks

Yang Lei[1,5], Xue Dong[1,5], Tonghe Wang[1,2], Kristin Higgins[1,2], Tian Liu[1,2], Walter J Curran[1,2], Hui Mao[2,3], Jonathon A Nye[3] and Xiaofeng Yang[1,2,4]

Published 4 November 2019 •
Physics in Medicine & Biology, Volume 64, Number 21

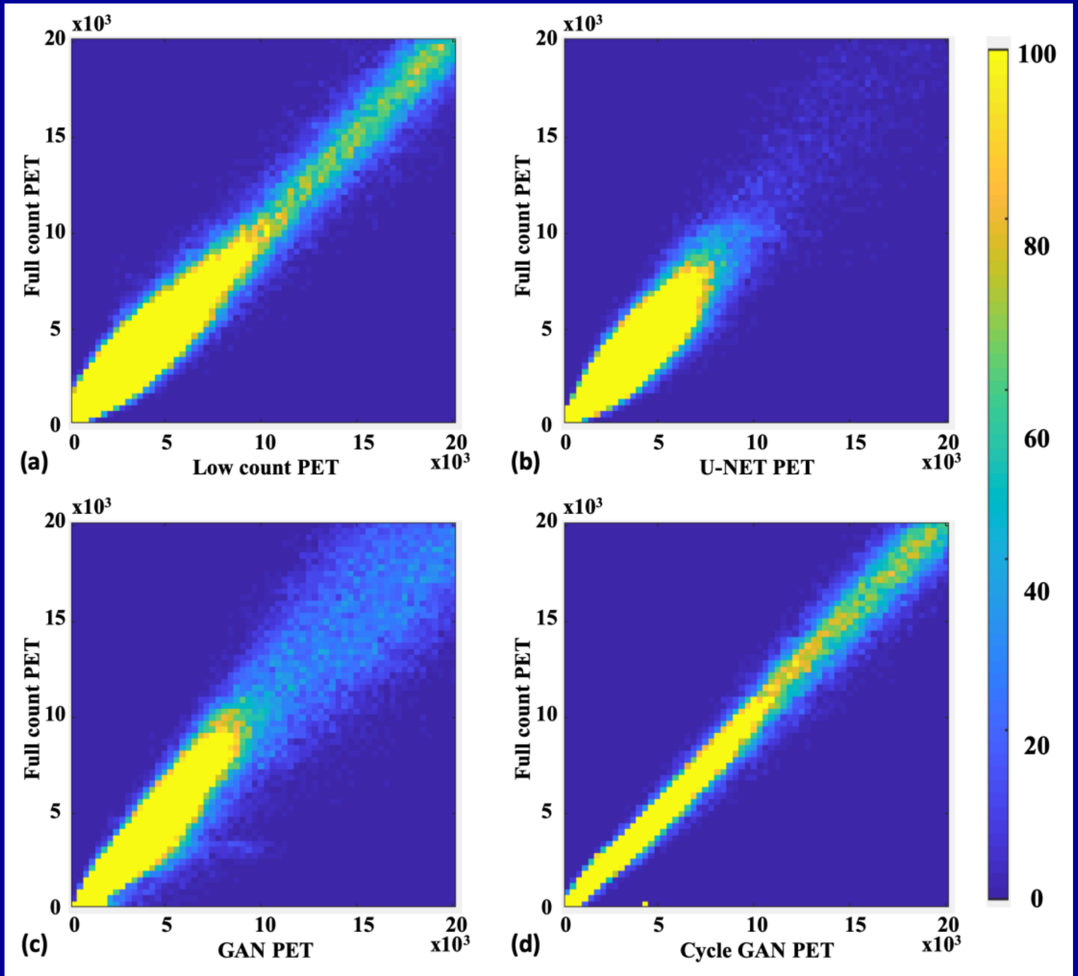

Low dose CT Imaging

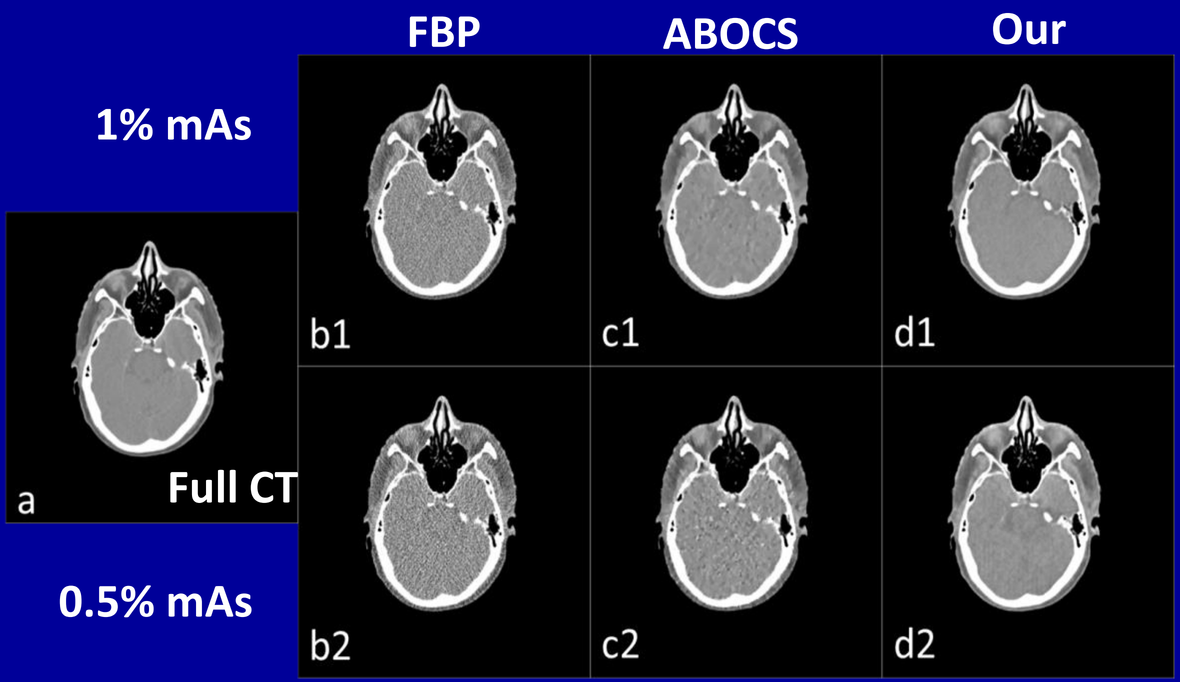

	% of full mAs	FBP	ABOCS	Our method	P-value FBP vs our method	P-value ABOCS vs our method
NMSE (%)	1%	1.97±0.44	1.71±1.31	1.14±0.61	<0.001	0.002
	0.5%	3.47±0.89	2.82±1.44	1.63±0.62	<0.001	<0.001
NCC (%)	1%	99.86±0.03	99.84±0.06	99.86±0.03	0.88	0.197
	0.5%	99.72±0.07	99.77±0.07	99.83±0.03	<0.001	0.008
Noise (HU)	1%	68.33±9.97	24.43±9.25	10.69±2.14	<0.001	<0.001
	0.5%	96.45±14.25	49.66±14.44	10.87±2.35	<0.001	<0.001
	reference	9.41±2.55				
CNR	1%	0.20±0.20	0.50±0.39	0.80±0.70	<0.001	0.025
	0.5%	0.13±0.13	0.28±0.25	0.85±0.58	<0.001	<0.001
	reference	1.20±0.80				
SNU (%)	1%	46.59±8.36	24.16±9.69	8.02±4.00	<0.001	<0.001
	0.5%	66.14±9.65	46.62±15.77	8.54±4.36	<0.001	<0.001
	reference	7.43±5.53				

Translator Disclaimer

Deep learning-based image quality improvement for low-dose computed tomography simulation in radiation therapy

Tonghe Wang; Yang Lei; Zhen Tian; Xue Dong; Yingzi Liu; Xiaojun Jiang; Walter J. Curran; Tian Liu; Hui-Kuo Shu; Xiaofeng Yang

Author Affiliations +

J. of Medical Imaging, 6(4), 043504 (2019). https://doi.org/10.1117/1.JMI.6.4.043504

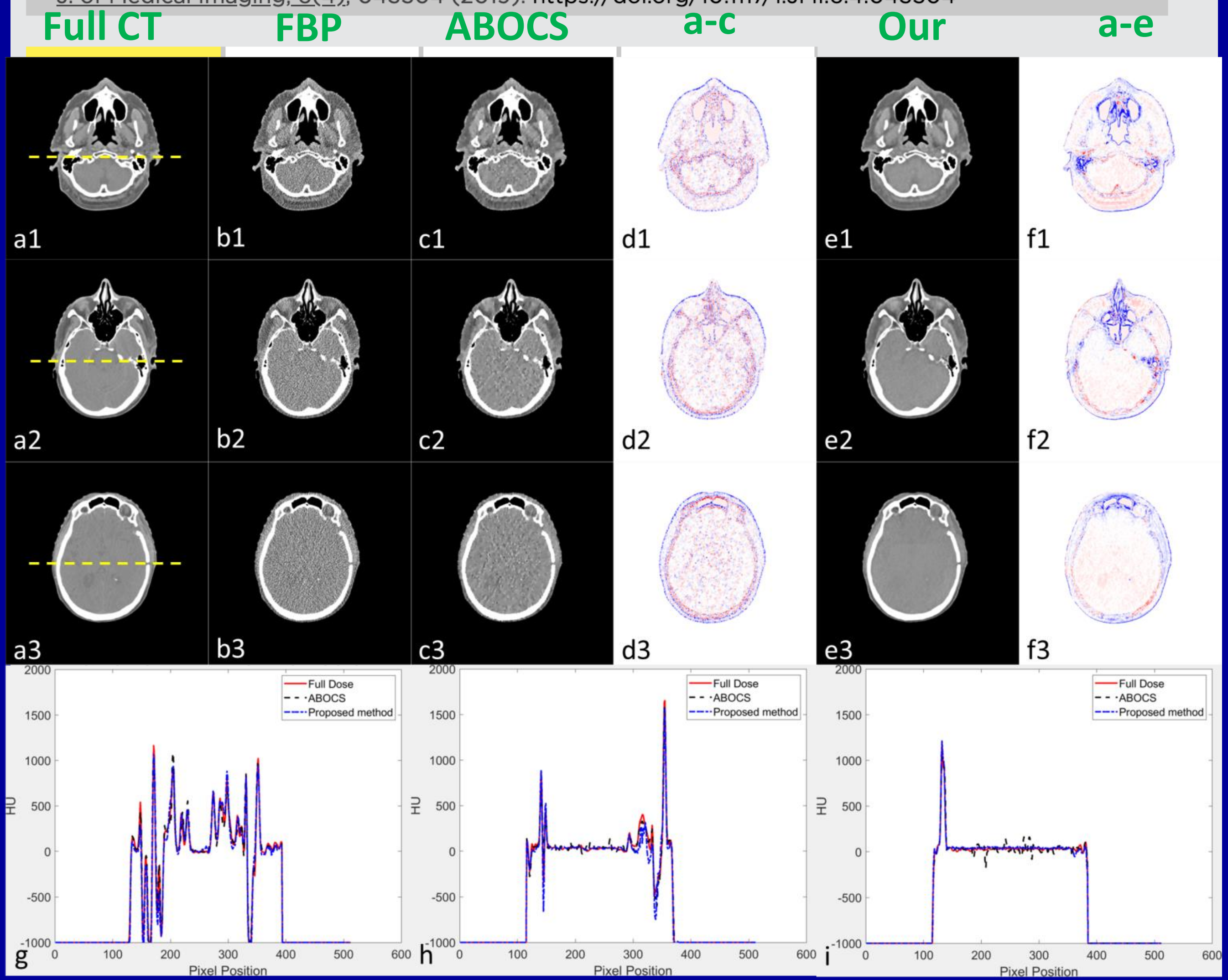

High Quality Proton Portal Imaging (PPI) Aided by DRR

High quality proton portal imaging using deep learning for proton radiation therapy: a phantom study

Serdar Charyyev[1], Yang Lei[1], Joseph Harms[1], Bree Eaton[1], Mark McDonald[1], Walter J Curran[1], Tian Liu[1], Jun Zhou[1], Rongxiao Zhang[2] and Xiaofeng Yang[1,3]

Published 27 April 2020 • © 2020 IOP Publishing Ltd
Biomedical Physics & Engineering Express, Volume 6, Number 3

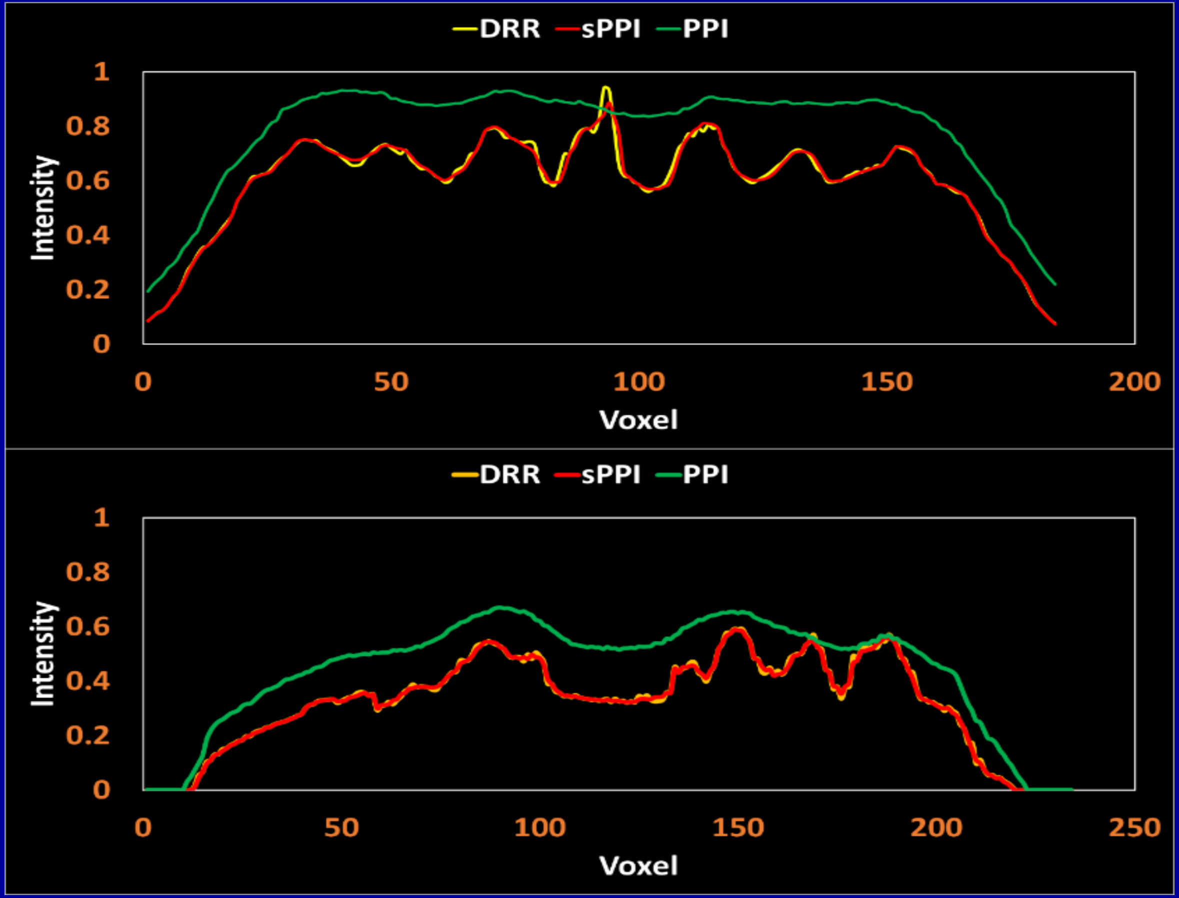

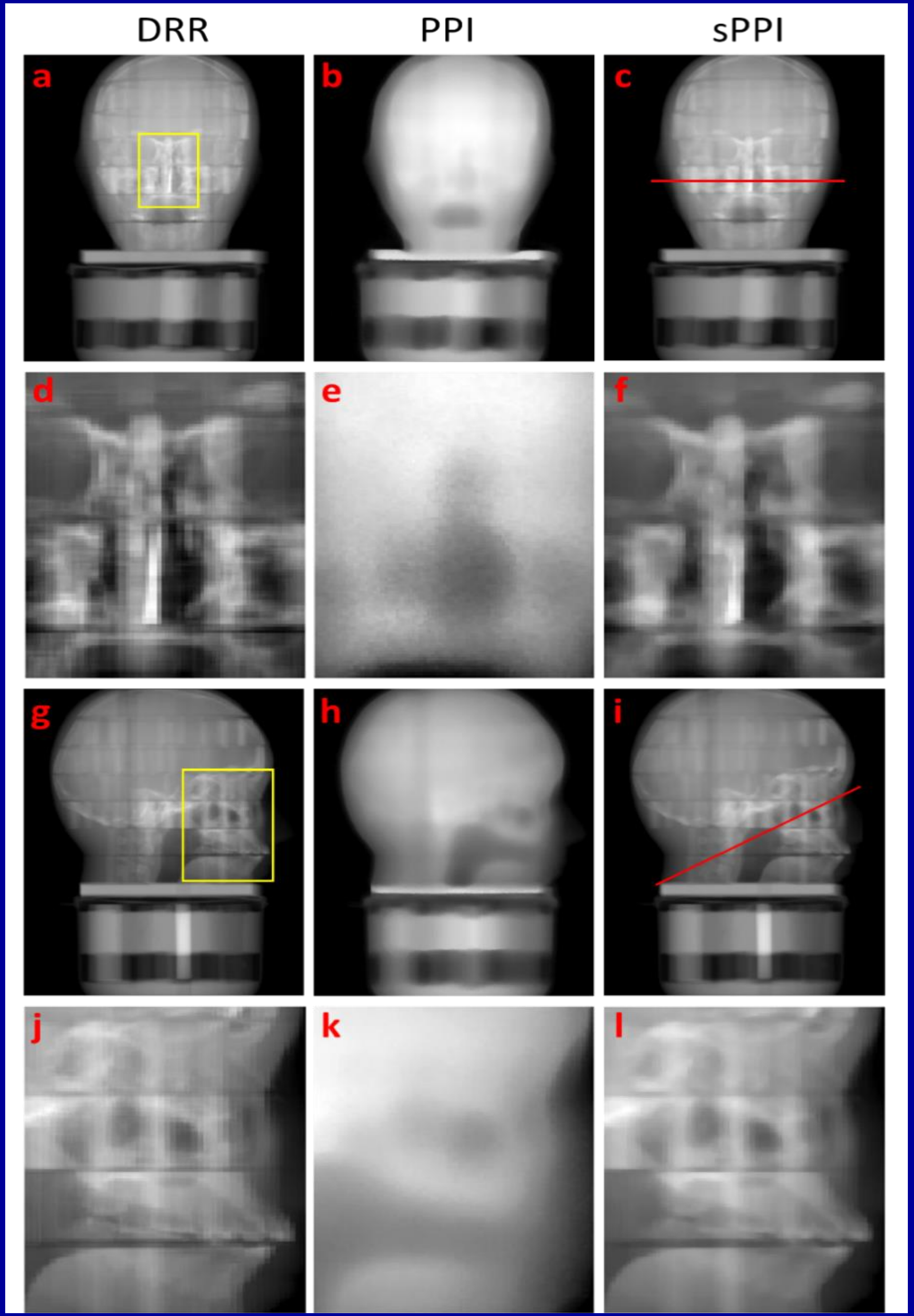

Deep-Self-Supervised High-Resolution CT Imaging

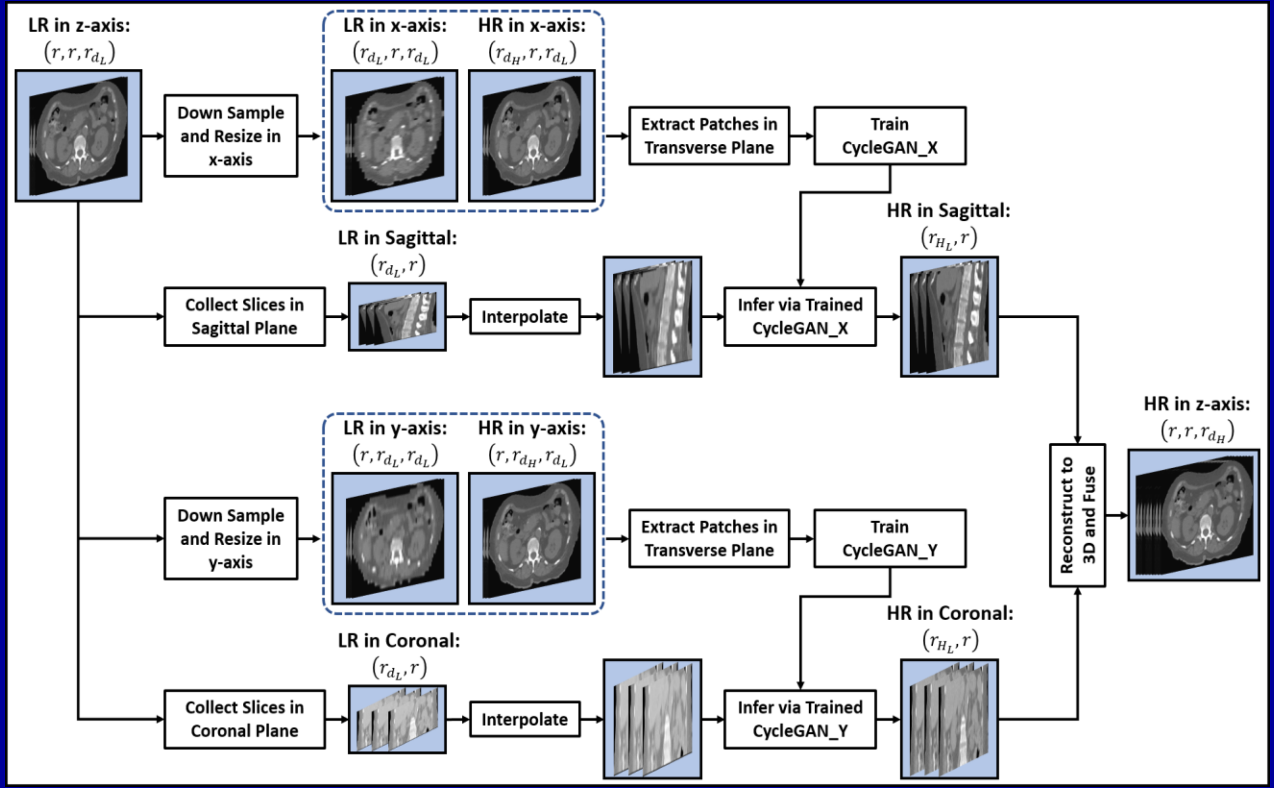

	MAE (HU)	PSNR (dB)	NCC
Bicubic	39.8±5.0	25.4±2.7	0.962±0.006
Proposed	23.2±4.9	34.5±2.8	0.997±0.001
P-value	<0.001	<0.001	<0.001

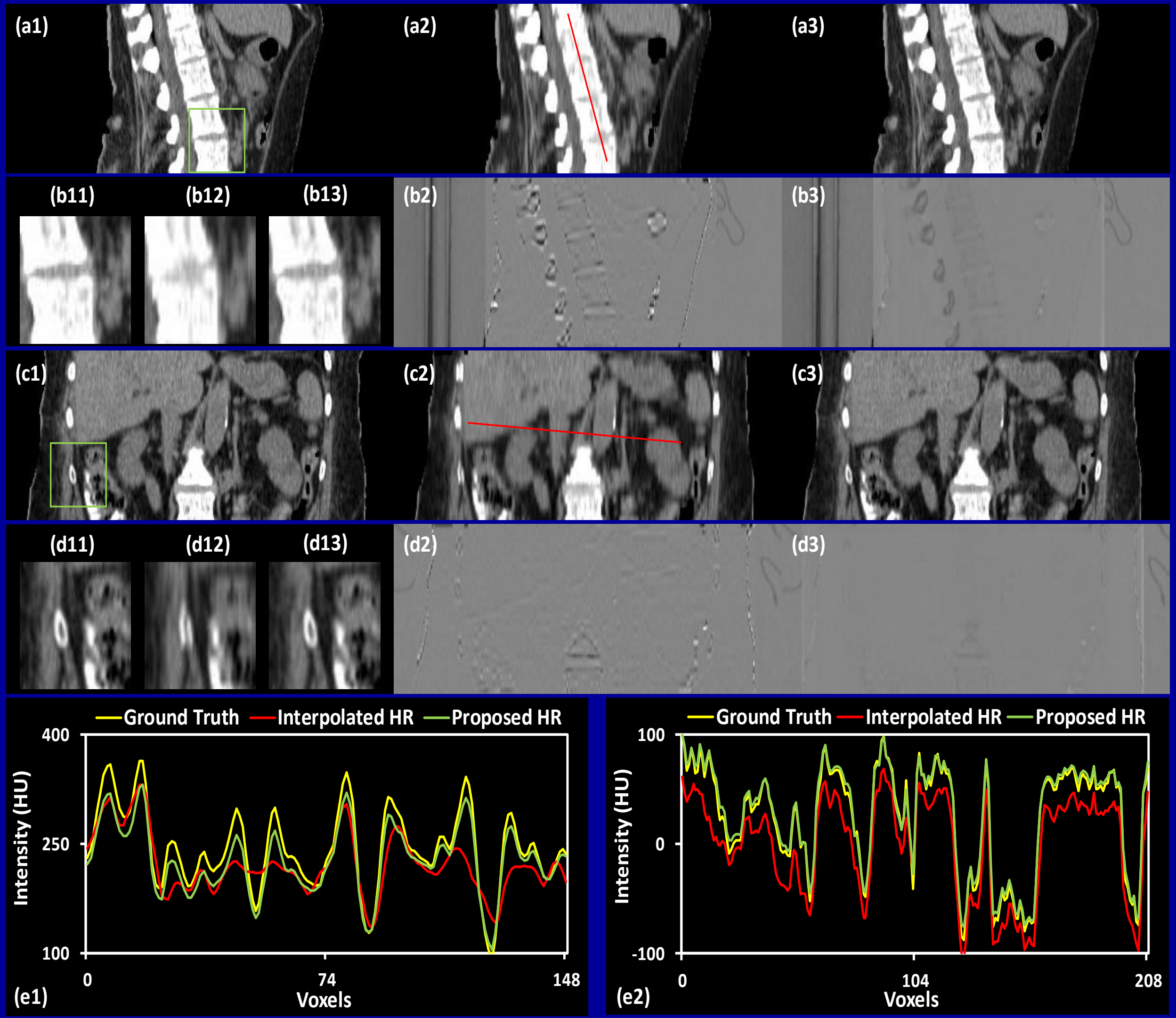

Lei Y, … Yang X, “A Patient-Specific Deep-Self-Supervised High-Resolution Method for CT Imaging”, 2020 AAPM Meeting (PO-GeP-M-33).

3D Volumetric Image Generation from 2D Projection Image

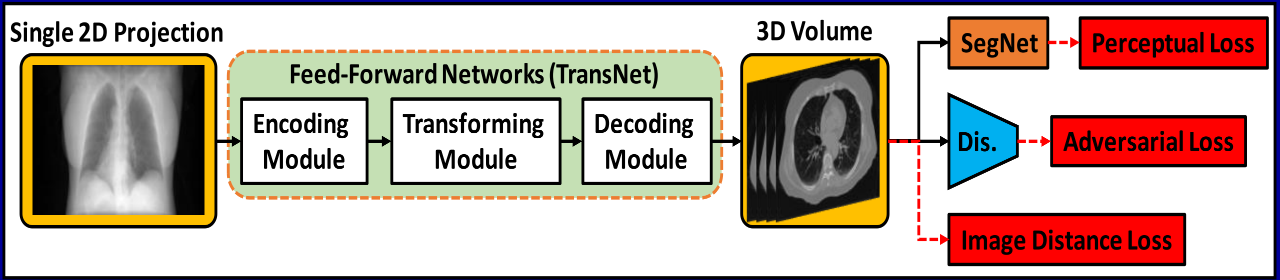

	0°	30°	60°	90°	Mean ± Std
MAE (HU)	90.6±15.5	105.3±14.1	97.5±9.2	103.9±11.6	99.3±14.1
NMAE	0.029±0.008	0.034±0.008	0.031±0.006	0.033±0.006	0.032±0.007
PSNR (dB)	24.1±2.4	23.1±2.2	23.5±2.0	23.0±1.9	23.4±2.2
SSIM	0.956±0.012	0.944±0.012	0.951±0.008	0.944±0.009	0.949±0.012

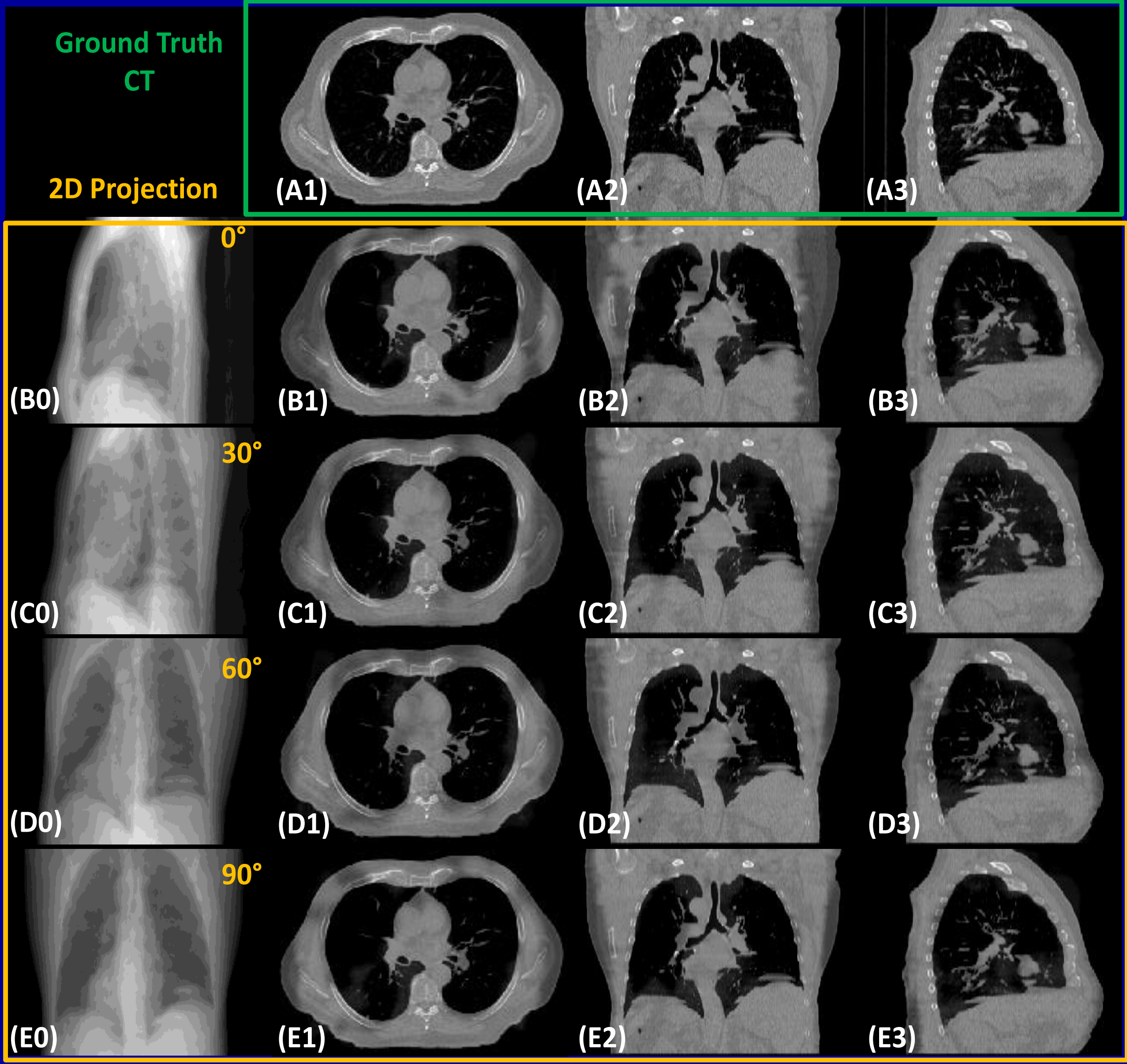

Lei Y, Tian Z, … Yang X, *2020 AAPM Meeting* (WE-F-TRACK 2-2)

Lei Y, Tian Z, … Yang X, *arXiv:2005.11832*, 2020

Outline

- **Inter-modality**
  - MRI-based synthetic CT
  - CBCT-based synthetic CT
  - CBCT/CT-based synthetic MRI
  - PET-based synthetic CT
- **Intra-modality**
  - Low-quality to high-quality image synthesis
    - Non-AC to AC PET
    - Low-to-high dose PET or CT
    - Low-to-high resolution imaging
    - 2D-3D generation
  - Cross-sequence MRI synthesis
  - SECT-based synthetic DECT
  - CBCT-based relative stopping power map

Cross-Sequence MRI Synthesis

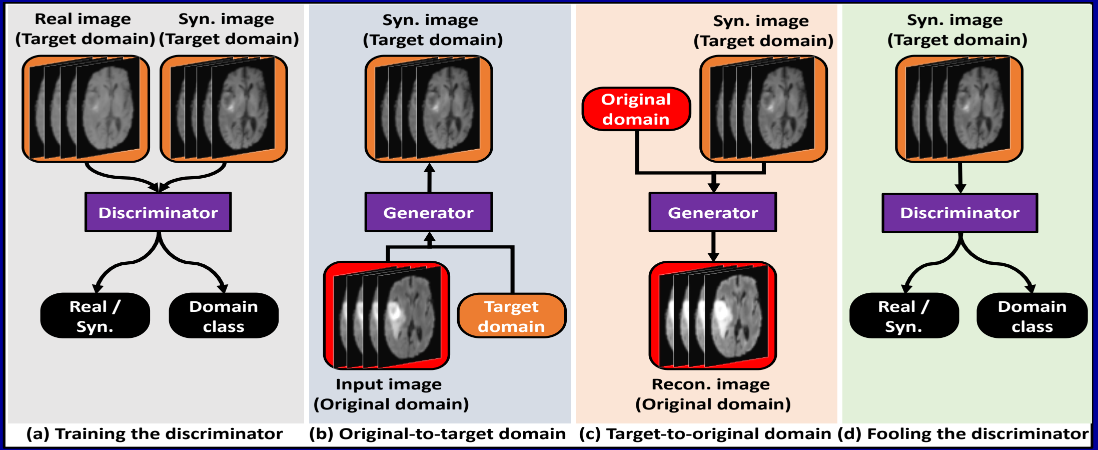

	T1	T1c	Flair
NMAE (%)	1.8±0.3	1.4±0.2	2.2±0.5
PSNR (dB)	30.1±3.7	36.3±3.5	30.4±4.7

Lei Y, ... Yang X, *Proc of SPIE*, 1131303, 2020

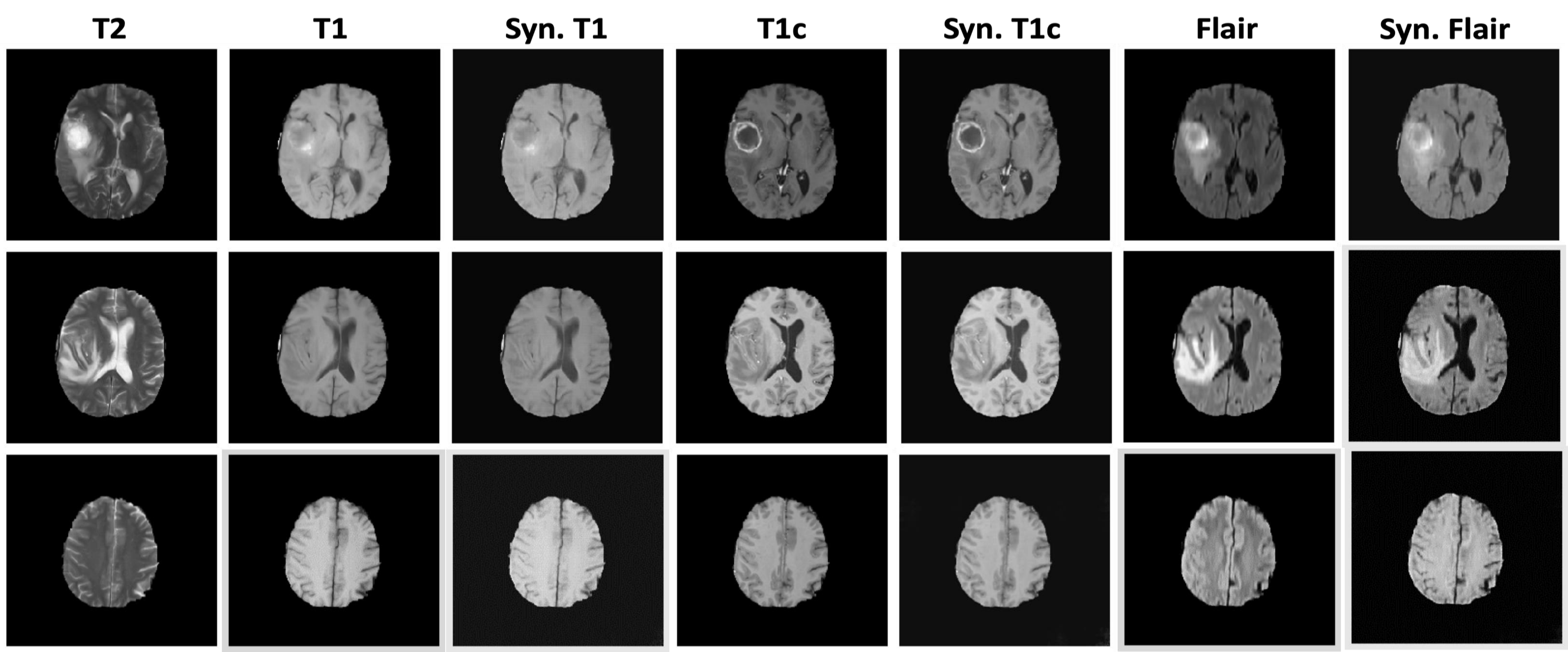

Synthetic Dual Energy CT (DECT) Imaging from Single Energy CT (SECT)

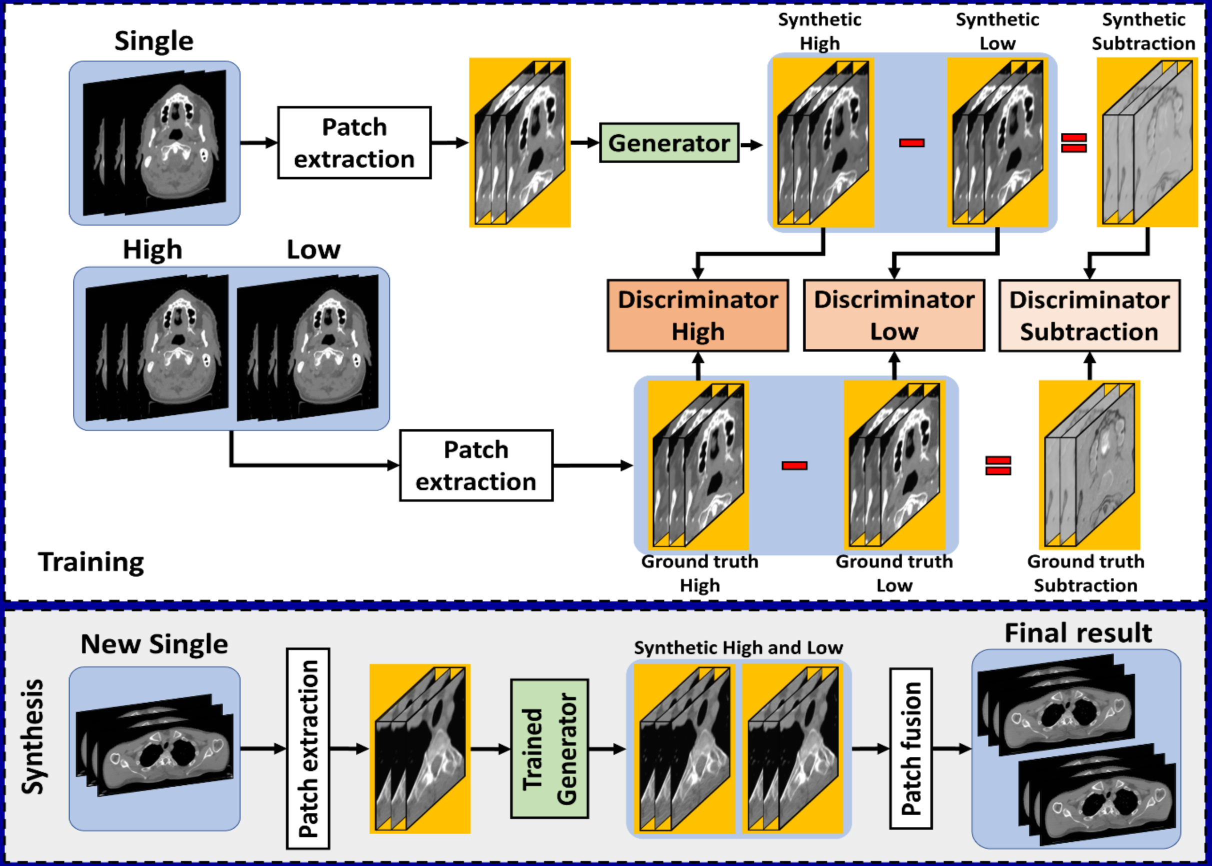

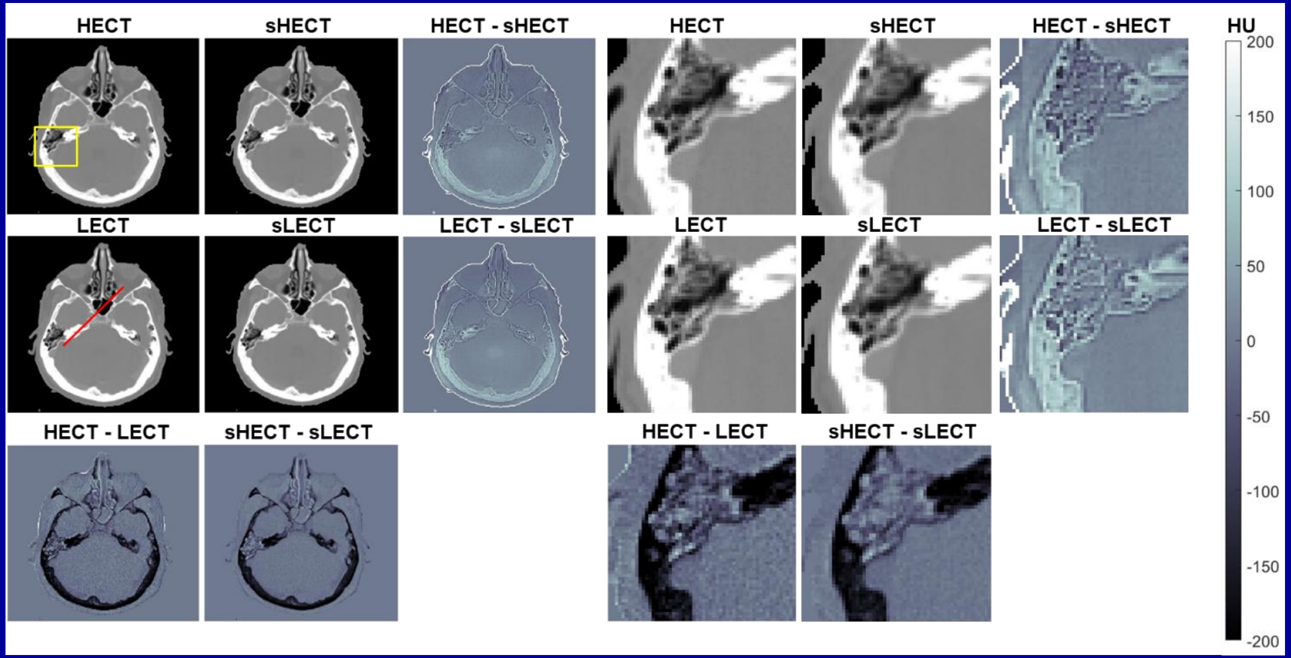

		sHECT	sLECT	sHECT-sLECT
MAE (HU)	Mean ± SD	30.23 ± 4.02	28.57 ± 5.03	16.05 ± 1.91
	Median	29.91	28.06	16.16
	Min	24.34	20.55	11.94
	Max	40.01	37.82	20.66
PSNR (dB)	Mean ± SD	31.83 ± 0.98	32.02 ± 1.11	33.19 ± 3.18
	Median	31.79	32.01	32.79
	Min	29.64	29.61	28.80
	Max	33.87	34.05	40.41
NCC	Mean ± SD	0.97 ± 0.01	0.97 ± 0.01	0.95 ± 0.008
	Median	0.97	0.98	0.95
	Min	0.94	0.95	0.93
	Max	0.98	0.99	0.96

Charyyev S, … Yang X. "Learning-Based Dual Energy CT Imaging from Single Energy CT for Proton Radiation Therapy," *arXiv:2003.09058*

CBCT-based Relative Stopping Power Map (RSPM)

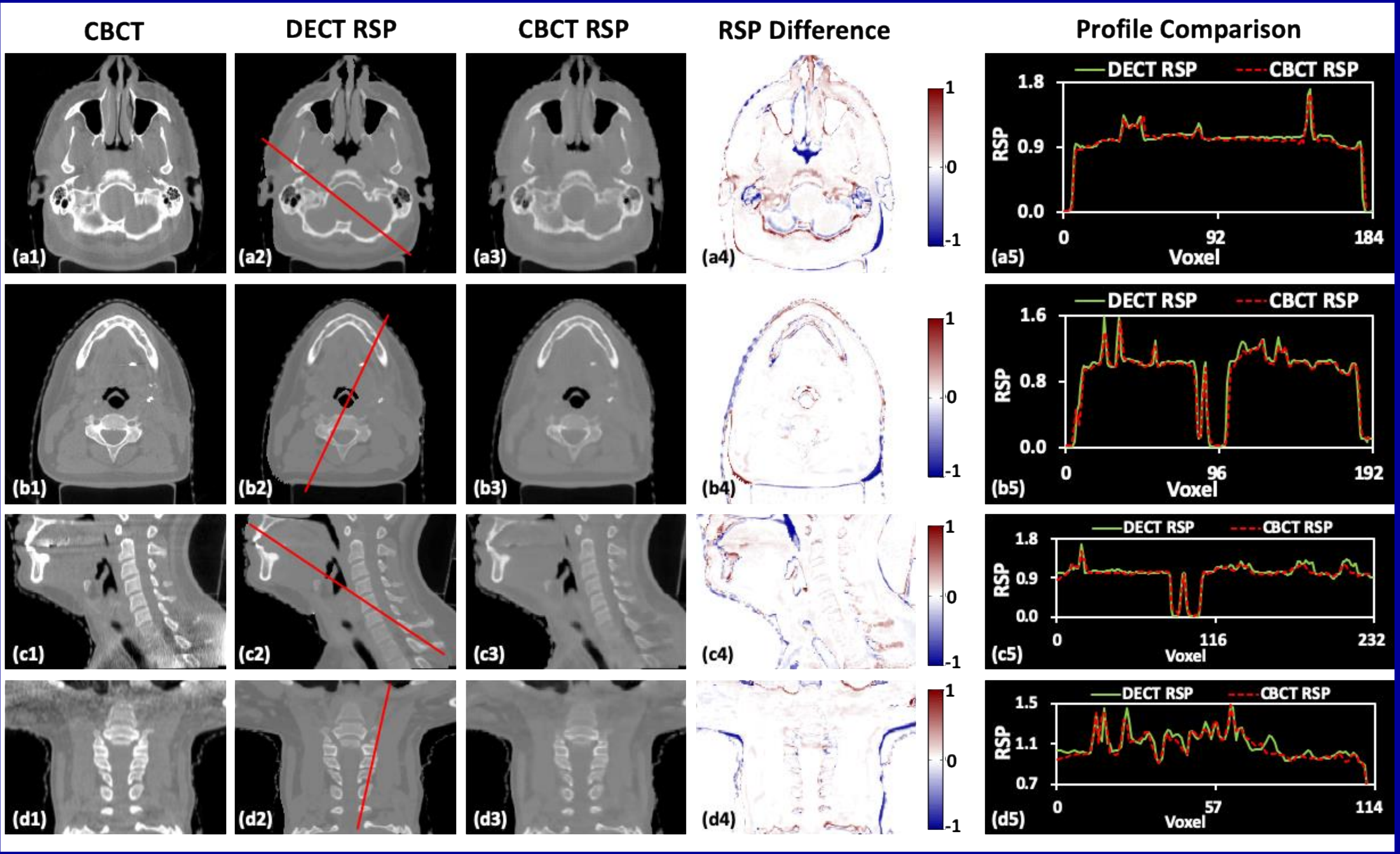

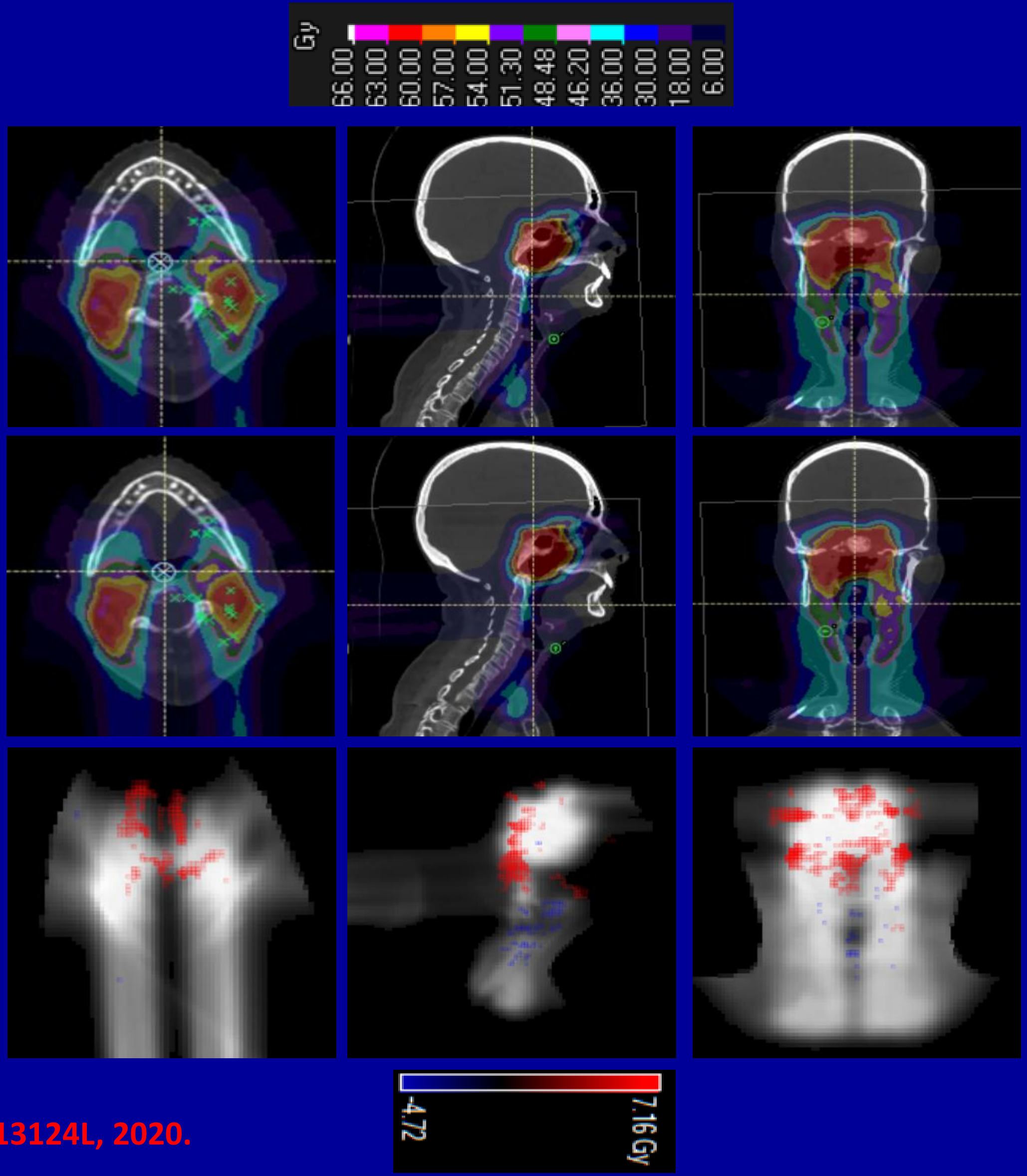

Harms J… Yang X. *Medical Physics,* 2020 (Major Revision).

Wang H, … Yang X. *Proc of SPIE,* 113124L, 2020.

Summary

- Promising work on inter-modality synthesis and intra-modality synthesis is being performed in image segmentation and registration, treatment planning, fast imaging, real-time tumor tracking and image-guided adaptive radiotherapy.
- To account for the potential unpredictable synthetic images that can be resulted by noncompliance with imaging protocols as training data, or unexpected anatomic structures, additional quality assurance (QA) step would be essential in clinical practice. The QA procedure would aim to check the consistency on the performance of the model routinely as well as the synthetic image quality of patient-specific case.
- To maximize the potentials and benefits of medical image synthesis in medical imaging and physics fields, it is critical to understand that a successful application depends as much on the nature of the task as on the nature of the synthesis algorithms, and the availability and quality of data.
- With the development in both artificial intelligence and computing hardware, more learning-based image synthesis methods are expected to facilitate the clinical workflow with novel applications.

Acknowledgements

- NIH NCI R01CA215718
- Varian AI Research Grant
- Emory Winship Prostate Research Pilot Grant

Q &A

EMORY
WINSHIP CANCER INSTITUTE
National Cancer Institute-Designated Comprehensive Cancer Center